AN EXPERIMENT TO SIMULATE THE TRAPPING AND DETECTION OF RADIOACTIVE ISOTOPES PRODUCED IN ICF IMPLOSIONS

By

Micah Christensen

A thesis submitted in partial fulfillment of the
requirements for the degree of

Bachelor of Science

Houghton College

January 2022

Signature of Author……..
Department of Physics
January 28, 2022

……
Dr. Mark Yuly
Professor of Physics
Research Supervisor

……
Dr. Brandon Hoffman
Professor of Physics

AN EXPERINEMT TO SIMULATE THE TRAPPING AND DETECTION OF RADIOACTIVE ISOTOPES PRODUCED IN ICF IMPLOSIONS

By

Micah Christensen

Submitted to the Department of Physics, Computer Science and Engineering
on January 28, 2022 in partial fulfillment of the
requirement for the degree of
Bachelor of Science

Abstract

It may be possible to measure the low energy nuclear cross sections of light ion reactions by trapping the reaction products from an ICF implosion and detecting their beta decays. To test this idea, an "exploding wire" experiment has been designed to simulate the expanding gas released in an ICF event. A copper plated tungsten foil was inserted into a vacuum chamber and activated with a deuteron beam via $^{65}Cu(d,p)^{66}Cu$. A current pulse then vaporized the copper to create an expanding radioactive gas, simulating the gas behavior in the ICF target chamber following the laser shot. Attempts were made to capture some gas and detect the ^{66}Cu beta decays using two trap designs, one using a getter foil and the other a turbopump. Results were obtained with both trap designs, using the Short-Lived Isotope Counting System (SLICS) consisting of plastic scintillator phoswich detectors and fast electronics to identify and count the beta particles.

Thesis Supervisor: Dr. Mark Yuly
Title: Professor of Physics

This material is based upon work supported by the Department of Energy [National Nuclear Security Administration] University of Rochester "National Inertial Confinement Program" under Award Number(s) DE-NA0004144.

TABLE OF CONTENTS

TABLE OF FIGURES

Chapter 1

ICF FOR NUCLEAR SCIENCE

1.1. Introduction

Inertial confinement fusion (ICF) is a process that reaches nuclear fusion conditions by rapidly heating and compressing a small fuel target capsule and is being considered as a new technique for studying nuclear science. In particular, ICF may be used to study low energy nuclear reactions, which are the kinds of reactions that occur naturally in stars. Fundamental measurements such as the nuclear cross section, which is proportional to the probability of a reaction occurring, may be made for several nuclear reactions. Nuclear cross sections may be used for testing stellar and big bang nucleosynthesis models but must be measured at the relatively low energies relevant for astrophysics.

ICF occurs at relatively low energies of keVs, making it a better choice than traditional particle accelerator techniques, which typically produce nuclear reactions at much higher energies of MeVs. The reason nuclear cross sections are traditionally measured at higher energies is because they are much more likely to occur at these energies. Very few nuclear cross sections have been measured below a few hundred keV, energies relevant for astrophysics, so nucleosynthesis models use nuclear cross sections that have been extrapolated from measurements made at much higher energies. The long-term goal of this research is to use ICF to measure the low energy nuclear cross sections for several light ion reactions of interest in astrophysics.

1.2. Nuclear Cross Section

Before discussing the proposed ICF experiment, it is necessary to explain the concept of nuclear cross sections. In general, nuclear reactions occur when two nuclei, or a nucleus and another subatomic particle, collide to produce one or more reaction products. Nuclear reactions can occur in hot dense plasmas like the sun or between energetic particles and targets in accelerator experiments. Nuclear cross sections, which describe how likely different reactions are to occur, are useful for testing stellar models and understanding the

structure of the nucleus and how nuclei and particles interact. The nuclear cross section of a reaction depends both on the energies of the interacting nuclei or particles, and their structure, meaning nuclear reactions have different probabilities of occurring between different nuclei and at different energies.

1.2.1. Cross Section Dependence on Energy

One reason the nuclear cross section depends on the energies of the colliding nuclei is because of interplay between the strong nuclear force and Coulomb repulsion. The strong nuclear force only comes into play when the nuclei get close enough, due to its short range. The distance between the nuclei must be on the order of 10^{-15} m, which is difficult to achieve because of the Coulomb repulsion between the protons in the nuclei. This repulsion presents a potential energy barrier, also called the Coulomb barrier [1], that the nuclei must overcome to get close enough for a reaction to occur. Classically, in order to overcome this barrier the nuclei are given a large amount of energy, typically on the order of MeV. When they lack the necessary energy, however, they can still interact by quantum tunneling through the barrier [1]. This second way is much less likely, meaning the cross sections are much smaller for low energy reactions (on the order of keVs). As an example, Figure 1 shows the Coulomb barrier with height V_B between a proton and a ^{40}Ca nucleus. Classically speaking, the proton and ^{40}Ca nucleus must have at least this much kinetic energy with respect to each other for a reaction to occur, but a reaction might still occur via quantum tunneling at a lower energy.

1.2.2. Light Ion Nuclear Reactions

Because the cross sections are much smaller at energies lower than the Coulomb barrier, they are often difficult to measure. Some low energy reactions have larger cross sections than others, however, making them easier to measure. These more probable low energy reactions occur between nuclei with the fewest protons, called light ions. The coulomb barrier height decreases with a decreasing number of protons and an increasing number of neutrons. Therefore, the most likely low energy reactions occur between isotopes of hydrogen such as deuterium and tritium, which each have only one proton and one and two neutrons, respectively.

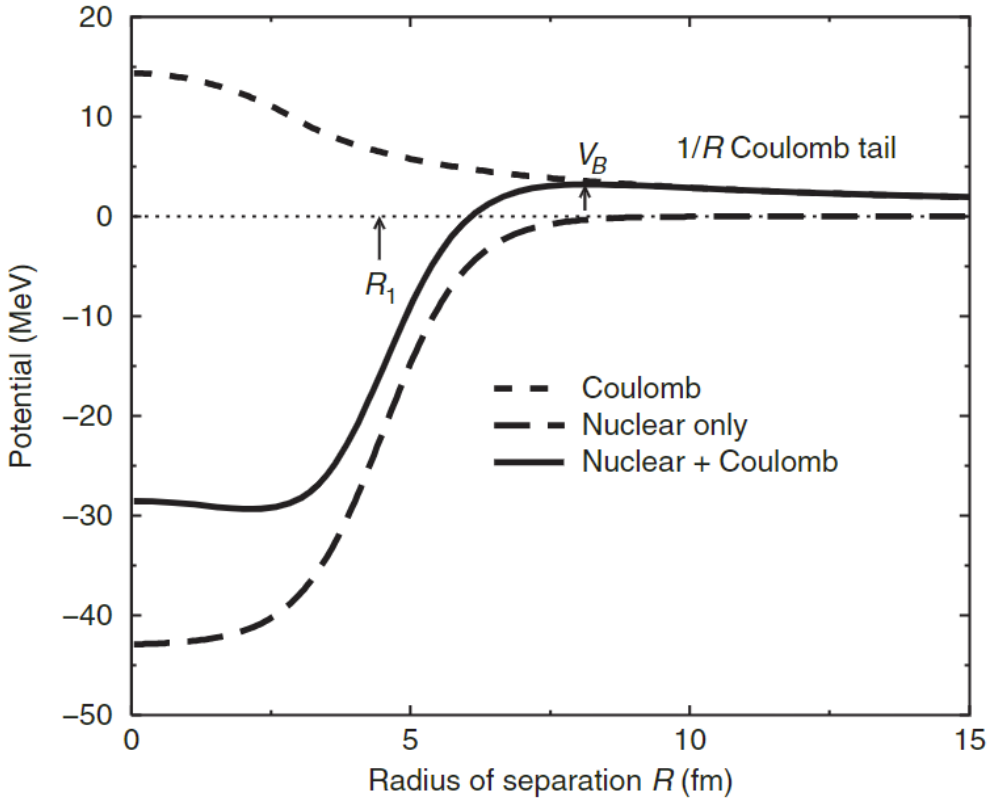

Figure 1. Coulomb barrier between a proton and ^{40}Ca nucleus. The potential energies, in MeV, of the Coulomb force, strong nuclear force, and combined forces (solid line), are given on the vertical axis. The distance of separation of the nuclei R, in fm, is given on the horizontal axis. The combined forces have a maximum energy $V_B \approx 3$ MeV, also known as the Coulomb barrier, which the nuclei must overcome to interact. For energies less than V_B, reactions are still possible via quantum tunneling through the Coulomb barrier. Figure taken from Ref. [1].

1.2.3. Nuclear Reactions of Interest

As a first step in measuring low energy nuclear cross sections, only the most likely reactions involving deuterium or tritium were considered. Based on this desired characteristic, several reactions have been proposed to study and are listed in Table 1. The reaction notation refers to traditional accelerator experiments, in which an accelerator is used to produce nuclear reactions when a beam of incident particles strikes a target. A new nucleus is produced, and often there are some other particles in the final state that can be detected. This is typically denoted as $A(a,b)B$, where A is the target nucleus, a is the incident particle, B is the residual nucleus, and b is the outgoing detected particle. The proposed reactions each use deuterium or tritium for the incident nuclei, and each reaction product is radioactive and decays by

emitting beta particles. Rather than detecting different types of *b* particles for each reaction, the beta decays from the different reaction products *B* can be detected for all the reactions of interest.

Table 1. Proposed reactions and product half-lives. The reactions of interest use deuterium or tritium for the incident nuclei. The reaction products are all radioactive and decay by beta emission with half-lives ranging from 20.2 ms to 7.13 s. Half-lives were extracted from the NNDC [2].

Reaction	Product Half-life	Reaction	Product Half-life	Reaction	Product Half-life
$^{3}H(t,\gamma)^{6}He$	807 ms	$^{9}Be(t,\gamma)^{12}B$	20.2 ms	$^{13}C(t,p)^{15}C$	2.45 s
$^{7}Li(t,\alpha)^{6}He$	807 ms	$^{10}B(t,p)^{12}B$	20.2 ms	$^{13}C(t,\gamma)^{16}N$	7.13 s
$^{6}Li(t,p)^{8}Li$	840 ms	$^{11}B(d,p)^{12}B$	20.2 ms	$^{14}N(t,p)^{16}N$	7.13 s
$^{9}Be(t,\alpha)^{8}Li$	840 ms	$^{13}C(t,\alpha)^{12}B$	20.2 ms	$^{15}N(d,p)^{16}N$	7.13 s

1.3. Motivation for Low Energy Nuclear Cross Sections

While many cross sections have been measured at higher energies, it is important to have measurements reaching down to the keV energy range as well, since these are especially important for stellar and cosmological models.

1.3.1. Never Previously Measured

The reason most low energy cross sections have not been previously measured is because traditional particle accelerator experiments essentially bombard a target nucleus with one particle at a time. The reaction products are then identified and counted to determine the cross section. Since the chance of a nuclear reaction occurring decreases dramatically with energy, the reaction rate is extremely low, and it takes a long time to produce a statistically adequate number of nuclear reactions. For the $^{7}Li(t,\alpha)^{6}He$ reaction, for example, an accelerator experiment with a 1 μA triton beam striking a 1.22 μm thick solid ^{7}Li target with an energy of 25 keV would take about 100 years to yield one million reactions, assuming the cross section for this reaction was about 10^{-8} mb [3]. Furthermore, accelerator labs are not equipped to safely accelerate tritium, which is radioactive and beta decays with a half-life of 12.32 years [2], contaminating accelerator beam lines.

1.3.2. Stellar and Big Bang Nucleosynthesis

Because many low energy nuclear cross sections have never been measured, cosmological models such as stellar and Big Bang nucleosynthesis rely on cross section values extrapolated from higher energies, which can lead to large uncertainties. These nucleosynthesis models describe the thermonuclear processes of lighter ions interacting to form heavier ions in stars and in the early universe. As described in Ref. [1], in Big Bang models, the average thermal energy of the universe was greater than 1 MeV during the first second, but cooled down to the keV energy range after about 2 s. At this time, there was a 250 s period where primordial nucleosynthesis occurred [1]. At the beginning of this time there were only protons and neutrons, and Figure 2 shows the predicted chain of nucleosynthesis reactions. In this model, the protons and neutrons interacted to form deuterons, the deuterons interacted with more protons or other deuterons to form tritons or ^{3}He nuclei, and these nuclei interacted with others to form even heavier ions. In Figure 2, this nucleosynthesis process continues until nuclei as heavy as ^{7}Be and ^{7}Li are formed.

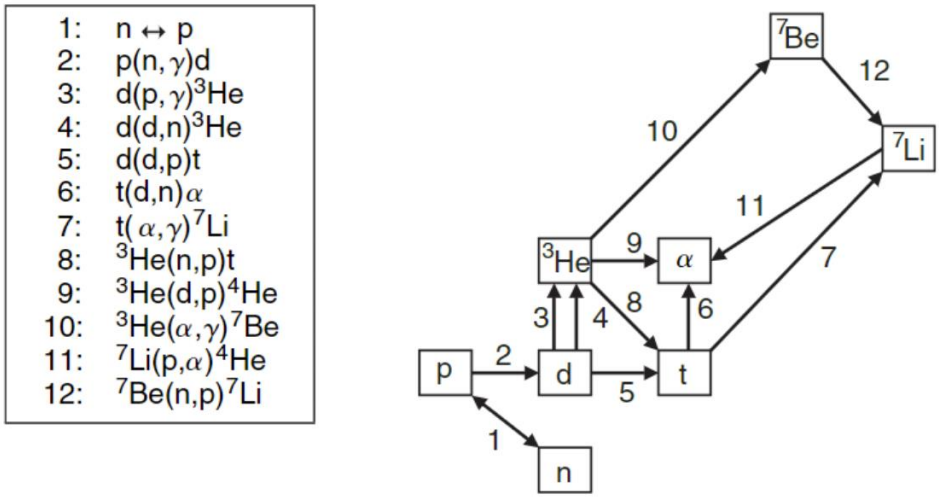

Figure 2. Predicted dominant reactions in primordial nucleosynthesis. At the beginning of the 250 s primordial nucleosynthesis period, there were only protons and neutrons. The average energy of the universe during this period was in the keV range, allowing reactions between the protons and neutrons, and eventually between their products, to occur. Figure taken from Ref. [1].

Big Bang nucleosynthesis models also predict elemental abundances over time based on the cross sections of reactions like those in Figure 2. An example is shown in Figure 3, which shows predicted abundances over time during the primordial nucleosynthesis period. In the

first 10 seconds there are primarily protons, neutrons, and some deuterons. Then ^{3}He and ^{4}He begin to form, followed by ^{7}Be and ^{7}Li, with some elements decreasing as they are used to form new elements.

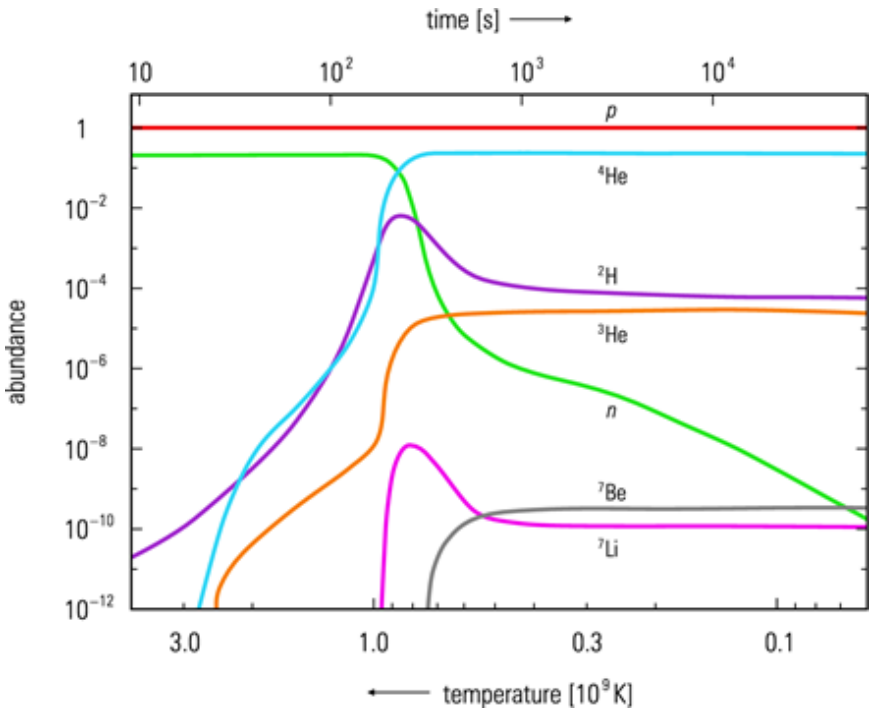

Figure 3. Elemental abundances over time. Bang nucleosynthesis models are used to predict the abundances of elements over time as the temperature of the early universe cools. The abundances of protons, neutrons, ^{2}H, ^{3}He, ^{4}He, ^{7}Be, and ^{7}Li are given. Figure taken from Ref. [4].

These models require as inputs accurate measurements of relevant low energy nuclear cross sections. Since many low energy cross sections have not been measured, extrapolations have been made from cross sections measured at higher energies in accelerator experiments. However, these extrapolations can lead to errors in nucleosynthesis models. For example, the abundance of ^{7}Li is overpredicted [5] while the abundance of ^{6}Li is underpredicted [3]. Measurement of the low energy cross section of the ^{3}H(t,γ)^{6}He reaction could help address this this problem since ^{6}He decays into ^{6}Li.

1.4. ICF as a Measurement Technique

Inertial confinement fusion (ICF) generates thermonuclear reactions similar to those in stars, making it a better choice than particle accelerators to measure the relevant low energy

nuclear cross sections. While a star confines the plasma in which nuclear reactions occur with gravity, ICF creates a plasma that is confined by its own inertia for a very short period of time. This is done by rapidly heating deuterium or tritium fuel in a target capsule to hundreds of millions of K, creating a high density plasma which implodes and is confined for less than a nanosecond. In this short period of time, despite the low energy, there can still be a large number of reactions since there are so many interacting nuclei in the macroscopic target. For comparison, if a tritium-filled SiO_2 "exploding pusher" target capsule was doped with 1% of ^{7}Li, the same $^{7}Li(t,\alpha)^{6}He$ reaction at an ion temperature of 18.3 keV could yield about one million reaction products in just 0.1 ns in a high-yield OMEGA laser shot [6], rather than the 100 years it might take for a particle accelerator experiment.

There are two methods of heating the target capsule in ICF, both of which involve powerful lasers. These are the indirect drive and the direct drive methods. The indirect drive method is mainly used at the National Ignition Facility (NIF) [7], associated with the Lawrence Livermore National Laboratory (LLNL) in California. This facility is capable of producing up to 1.8 MJ of UV energy and consists of 192 laser beams of dimensions 40 cm by 40 cm [8]. In the indirect drive method, an approximate 1 mm diameter spherical target is placed inside a gold cylindrical shell called a hohlraum [9]. The laser light enters the ends of the hohlraum and is absorbed by the gold, which emits x rays that symmetrically heat the target. In the direct drive method, rather than generating x rays, the laser beams directly strike the target capsule. This method is mainly used by the OMEGA laser system at the Laboratory for Laser Energetics (LLE) [10] at the University of Rochester in New York.

1.4.1. OMEGA Laser System

The OMEGA laser system uses 60 laser beams to symmetrically heat the target capsule and is capable of delivering up to 30 kJ of energy to the target in about 1 ns. The facility housing the laser system stands about 10 m tall and 100 m in length and is shown in Figure 4. The general ICF process of either the indirect or direct drive method is shown in Figure 5, where the lasers are used to rapidly heat the outer layer of the target to hundreds of millions of K, causing it to ablate, or blow off like a rocket. This ablation sends shockwaves inward that

cause the target to implode, compressing the fuel to hundreds of g/cm^3. At these temperatures and densities, thermonuclear reactions can occur.

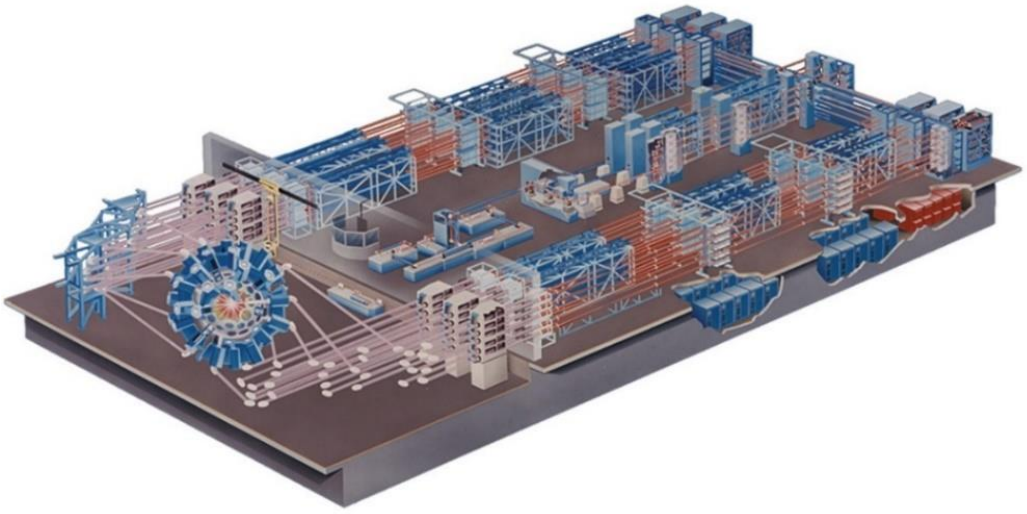

Figure 4. OMEGA laser system. The laser bay stands about 10 m tall and 100 m in length. Three UV lasers are split and amplified into 60 laser beams, which are focused down to strike an approximately 1 mm diameter spherical DT fuel capsule. The beam amplification systems are toward the right and the target chamber is toward the left. This heats and compresses the fuel to stellar temperatures and densities, allowing thermonuclear reactions to occur. Figure taken from Ref. [9].

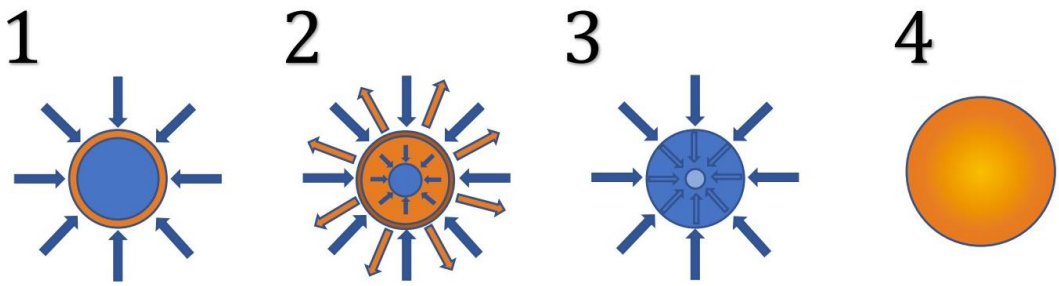

Figure 5. ICF process. (1) The laser beams in the direct drive method or x-rays in the indirect drive method strike the target capsule. (2) The outer layer of the capsule is rapidly heated and ablates. (3) The opposite and equal reaction force from the outer layer ablation sends shockwaves inward that cause the target mixture to implode. (4) Once heated to hundreds of millions of K and compressed to hundreds of times the liquid density, thermonuclear reactions occur. Figure taken from Ref. [6].

After an ICF implosion, the reaction product ions cool, recombine, and expand outward in a neutral gas. The nuclear cross sections can be measured by collecting a fraction of the reaction products in the expanding gas, and for the proposed reactions of Table 1, detecting their beta decays. This fraction may be very small, however, so to detect a statistically adequate number of reaction products, the nuclear reaction yields would need to be large enough. The predicted yields of the proposed reactions [11] are shown in Table 2. The yields were based on parameters from OMEGA shot 77951, which used a SiO_2 "exploding pusher" target capsule filled with a 1.5%-98.5% deuterium tritium mixture reaching an energy of 18.3 keV. Reactivities were calculated using TALYS-1.9 and S-factor extrapolations of Abramovich et. al. [13]. The most promising reactions are highlighted in orange, with yields on the order of 10^4 to 10^6 reaction products.

1.4.2. Proposed ICF Experiment

In order to detect the reaction products resulting from an ICF implosion, the expanding reaction products must be trapped shortly after the implosion, since the most prominent reaction products decay with sub second half lives. A detector able to identify beta particles must be placed near the trap to detect the decays of the reaction products. Assuming the efficiencies of the traps and detectors are known, then the total number of reactions that occurred can be determined, which is necessary for measuring the nuclear cross sections.

In addition to the reaction products, an electromagnetic pulse (EMP), neutron pulse, and x-rays are also produced within nanoseconds after the laser shot. The detectors used to count the beta decays of the reaction products are sensitive to this prompt radiation, however, so they must be turned on only after it has passed. This will avoid large background radiation counts as well as possible damage to the detectors. A general timeline for a proposed experiment is shown in Figure 6, where the initial radiation is produced within the first 10 ns and the electronics and detectors are turned on "long after" this prompt radiation, 1 to 2 ms after the shot. The detectors, which are plastic scintillator detectors that emit flashes of light which get converted to current pulses by photomultiplier tubes (PMT), will be discussed more fully in the Chapter 3.

Table 2. Predicted ICF yields for reactions of interest. The predicted yields are based on the parameters of OMEGA shot 77951, which used a SiO_2 target capsule filled with a 1.5%-98.5% DT mixture reaching an energy of 18.3 keV. Reactivities were calculated using TALYS-1.9 [12] and the S-factor extrapolations of Abramovich et. al. [13]. Since there is no cross section available for the $^{3}H(t,\gamma)^{6}He$ reaction, the predicted yield was based on assuming a branching ratio of 10^{-7}, which was a "best case" estimate. Table taken from Ref. [14].

Reaction	Product Half-life	Reactant Abund.	Predicted Yield
$^{3}H(t,\gamma)^{6}He$	807 ms	^{3}H fill	8×10^{4}
$^{6}Li(t,p)^{8}Li$	840 ms	7.6%	$4\text{-}16\times10^{5}$
$^{7}Li(t,\alpha)^{6}He$	807 ms	92.4%	$1\text{-}4\times10^{5}$
$^{9}Be(t,\alpha)^{8}Li$	840 ms	100%	8×10^{4}
$^{9}Be(t,\gamma)^{12}B$	20.2 ms	100%	3.0
$^{10}B(t,p)^{12}B$	20.2 ms	19.9%	923
$^{11}B(d,p)^{12}B$	20.2 ms	80.1%	1735
$^{13}C(t,\gamma)^{16}N$	7.1 s	1.1%	0.1
$^{13}C(t,\alpha)^{12}B$	20.2 ms	1.1%	108
$^{13}C(t,p)^{15}C$	2.45 s	1.1%	17.7
$^{14}N(t,p)^{16}N$	7.1 s	99.6%	2.5
$^{15}N(d,p)^{16}N$	7.1 s	0.4%	2.0

1.4.3. Trap and Detector Systems

Two trap and detector systems have been proposed to collect the expanding reaction products and detect their beta decays. One uses a turbopump for its trap and the other uses a getter. As shown in Figure 7, the turbopump trap uses a long collection tube with one end placed close to the target capsule in the center of the target chamber. After the implosion, some of the expanding reaction products enter the collection tube. A turbopump outside the chamber, attached to the other end of the tube, traps the reaction products in a box-shaped

detector. Once trapped in this hollow rectangular prism plastic scintillator detector, the product nuclei decay, emitting beta particles that pass through the walls of the detector. The scintillator emits flashes of light that are seen by a PMT optically coupled to one end of the detector system.

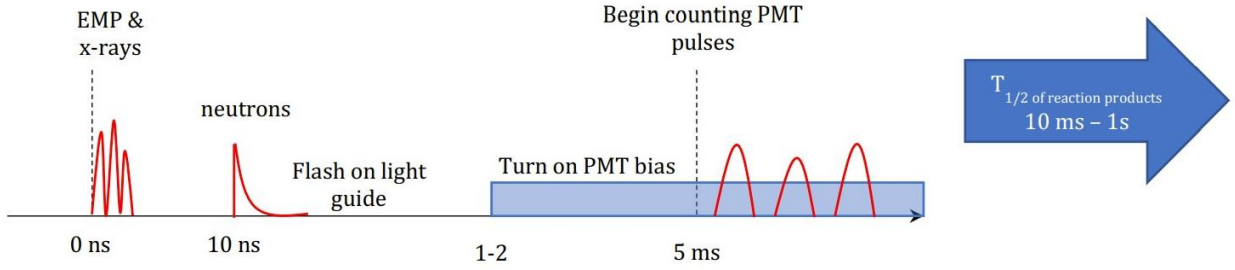

Figure 6. Timing diagram for the proposed ICF experiment. Immediately after the ICF laser shot, an EMP and x-rays are produced. The reaction products of interest are produced in the implosion, as well as neutrons from the DT reaction. "Long after" the initial radiation, the PMT bias is turned on and counting begins as the beta decays of the reaction products are detected.

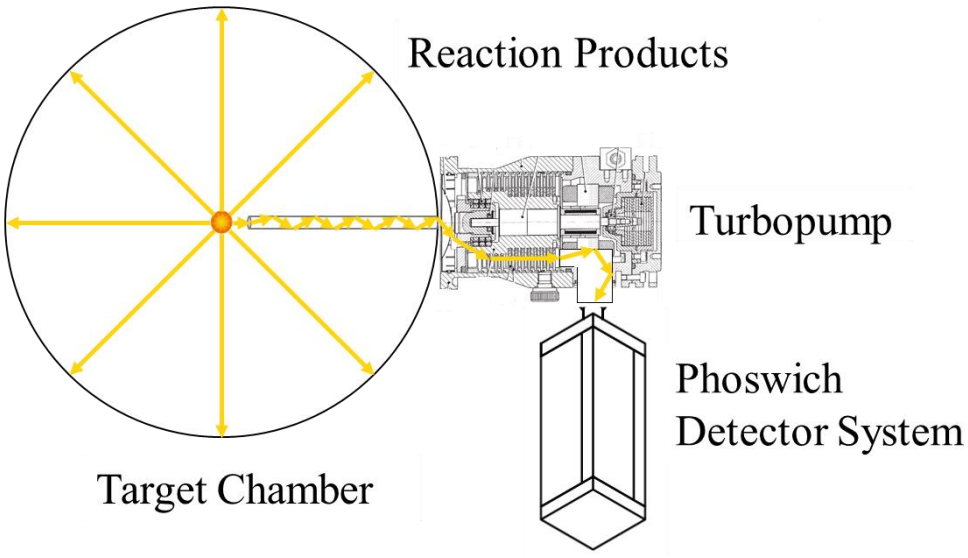

Figure 7. Turbopump trap and detector system. After the ICF implosion, the expanding reaction products enter a collection tube. This leads to a turbopump that pushes them into a box-shaped phoswich detector system, where they are trapped, and their decays are detected.

As shown in Figure 8, the getter trap uses a foil to which the reactions products will stick. The getter foil will be placed close to the target, capturing as many expanding product nuclei as possible. Since the reaction products are still ionized immediately after the implosion, a high voltage could be applied on the opposite side of the target to propel even more reaction products toward the getter. A small plastic scintillator detector placed directly behind the getter foil will detect the emitted beta particles from the trapped product nuclei. A light guide would be used to transmit the light from the plastic scintillator detector to the PMT safely outside the target chamber.

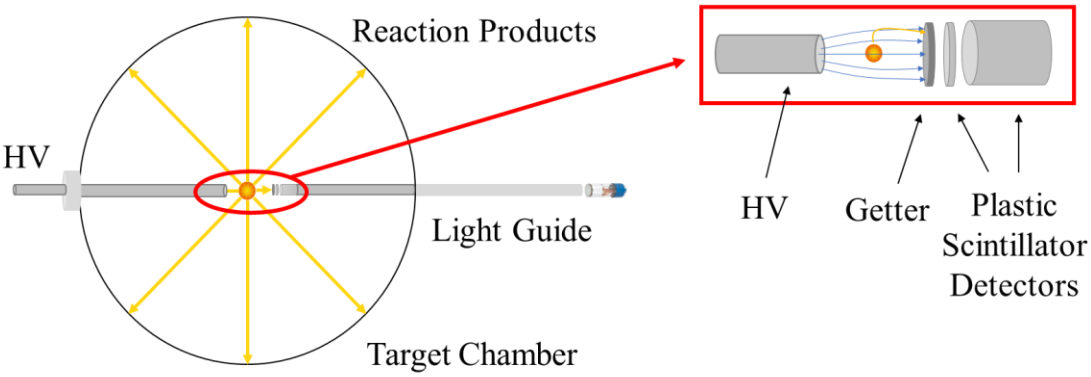

Figure 8. Getter trap and detector system. The expanding reaction products stick to a getter, with a phoswich detector system placed directly behind it. A high voltage could be applied to the opposite side of the target to propel even more of the ionized reaction products toward the getter. A light guide would be used to transmit the light from the plastic scintillator detectors to a PMT outside the target chamber.

For naturally "sticky" products, the getter foil is more advantageous than the turbopump trap, as sticky products will likely stop in the collection tube or turbopump before reaching the box-shaped detector. Inert gases, on the other hand, may not stick to the getter foil, making the turbopump trap a better option. The feasibility of using either system, however, is yet to be determined.

1.5. Previous Work

Before ICF could be used to measure low energy nuclear cross sections using the getter and turbopump trap systems, several questions needed to be answered. The capabilities of detecting sub second half-lives, and furthermore trapping and detecting a radioactive beta-

emitting gas, needed to be demonstrated, the background rate of typical high yield OMEGA shots needed to be measured, and the fraction of trapped and detected product nuclei needed to be determined. An experiment to create and detect ^{6}He [15] was performed to answer the first question, an experiment to trap and detect radioactive ^{41}Ar gas [14,16] was carried out to answer the second question, an OMEGA ride-along experiment [16,17] was done to answer the third question, and the experiment described in this thesis was attempted to answer the last question.

1.5.1. ^{6}He Experiment

To test the capability of detecting sub second half-lives, an experiment was performed to create and detect ^{6}He, which is listed in Table 2 with an 807 ms half-life. In order to create ^{6}He, the tandem Pelletron accelerator at SUNY Geneseo was first used to strike a 0.36 mm thick polyethylene sheet with an approximately 110 nA beam of 2.0 MeV deuterons. Neutrons produced via ^{2}H(d,n)^{3}H then struck a 19.5 mm by 26 mm by 6.5 mm thick ^{9}Be plate located directly behind the deuterated polyethylene. The neutrons reacted with the ^{9}Be to produce ^{6}He via ^{9}Be(n,α)^{6}He. A detector similar to the detectors proposed for the ICF experiments was positioned directly behind the ^{9}Be plate, and the beta particles emitted from the embedded ^{6}He nuclei were detected. This experiment showed that reaction products with sub second half-lives could be successfully detected, answering the first question.

1.5.2. ^{41}Ar Gas Experiment

In order to test whether or not a radioactive gas could be trapped and detected, an experiment was performed using ^{41}Ar. Argon (^{40}Ar) gas was irradiated for 2 hours with a 4 nA beam of 2 MeV deuterons with the tandem Pelletron accelerator at SUNY Geneseo. This produced ^{41}Ar via the ^{40}Ar(d,p)^{41}Ar reaction, a radioactive isotope decaying by beta emission with a 109 minute half-life. The gas cell containing the ^{40}Ar and ^{41}Ar mixture was transported to a test chamber at Houghton College, to which the turbopump trap and detector system from Figure 7 was attached. The gas was released into the chamber and the turbopump system was used to trap and detect the ^{41}Ar nuclei. The results of the experiment showed

that the turbopump system could be used to successfully trap and detect radioactive beta-emitting gas, answering the second question.

1.5.3. OMEGA Ride-Along

To measure the expected background rate, both the getter detector and turbopump detector were used in an OMEGA ride-along experiment, where they were placed outside the target chamber for several high-yield shots, as shown in Figure 9. The detectors started collecting data just a few ms after the laser shots, and for some shots, lead bricks were placed in front of the detectors for extra shielding.

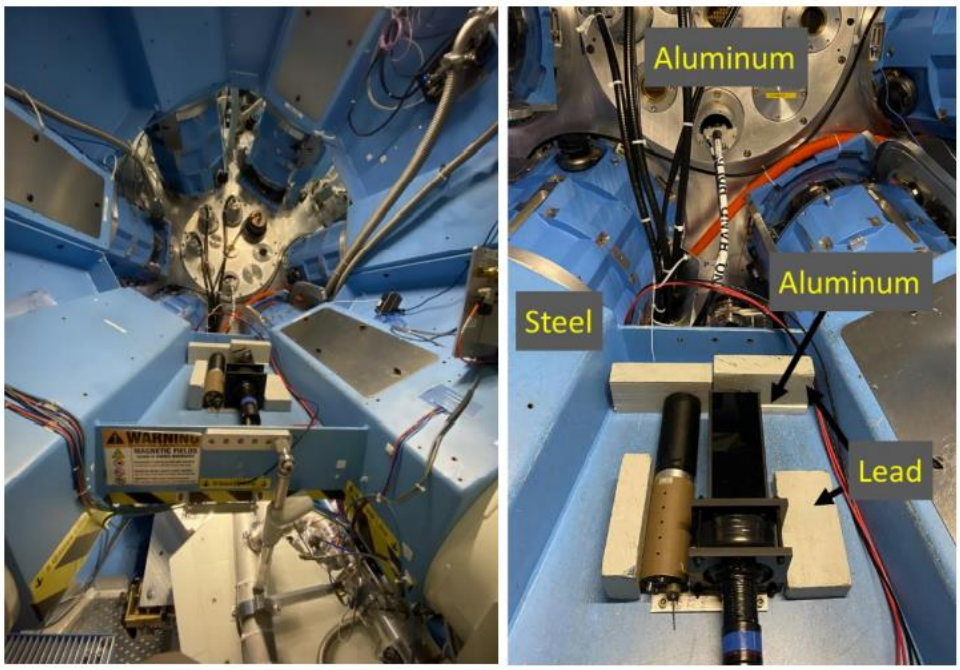

Figure 9. OMEGA ride-along experiment. The turbopump detector and getter detector were placed side by side on the H-10 webbing about 2.4 m from the target chamber center. They were held in place by an aluminum plate bolted to the platform, with lead blocks pressed against either side.

Results from OMEGA shots 96181 and 96184 are shown in Figure 10. The turbopump detector was used in these experiments with no shielding. Shot 96181 had a neutron yield of 1.32×10^{14} with an ion temperature of 8.44 keV and shot 96184 had a neutron yield of 1.56×10^{14} with an ion temperature of 10.64 keV. The background rates detected by the turbopump detector reached over 350,000 events per second and the electronics were

unable to keep up with the high count rate, leaving "gaps" in the data. The electronics could be set to collect data for different amounts of time before reading it out, and this collection time affected the size of these gaps, as shown in Figure 10.

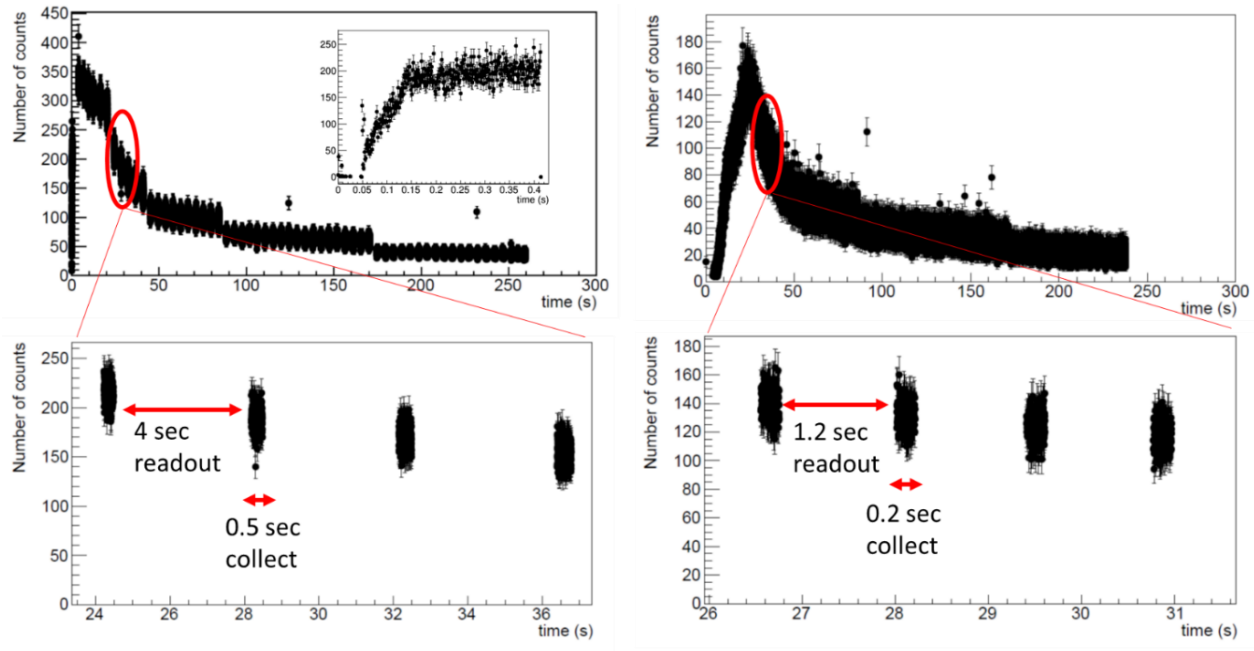

Figure 10. Results from turbopump detector in the OMEGA ride-along experiment. The decay curves for shots 96181 and 96184 are shown on the left and right, respectively. The background rates reached over 350,000 events per second and the electronics for the detectors had trouble keeping up, leaving "gaps" in the data.

Results from shot 96188 are shown in Figure 11, where the getter detector was used with lead shielding. The volume of the getter detector was much smaller than the turbopump detector, so the background count rate was much lower, reaching only about 18,000 events per second. The electronics could more easily keep up with this lower count rate, leaving fewer gaps in the counts vs. time graphs.

From these initial results, the background rate appeared to be low enough for experiments involving the getter detector but too high for experiments involving the turbopump detector. From the assumption that the trap and detector systems would collect about 1% of all reaction products with 100% efficient detectors, then for a one-second half-life product with a yield similar to the highest yields of Table 2, the number of decays in the first half-life would

be 500 to 50,000 [16]. In order to have a reasonable signal-to-noise ratio, then, the background must be approximately within or less than this range. However, in the actual experiments, the getter detector would be inside the target chamber, possibly exposed to more background radiation, and the turbopump detector may have more shielding, giving less background radiation. Overall, the background may be low enough for a successful experiment, but future ride-along experiments with improved electronics and shielding would be important in confirming this as well as determining the sources of background radiation.

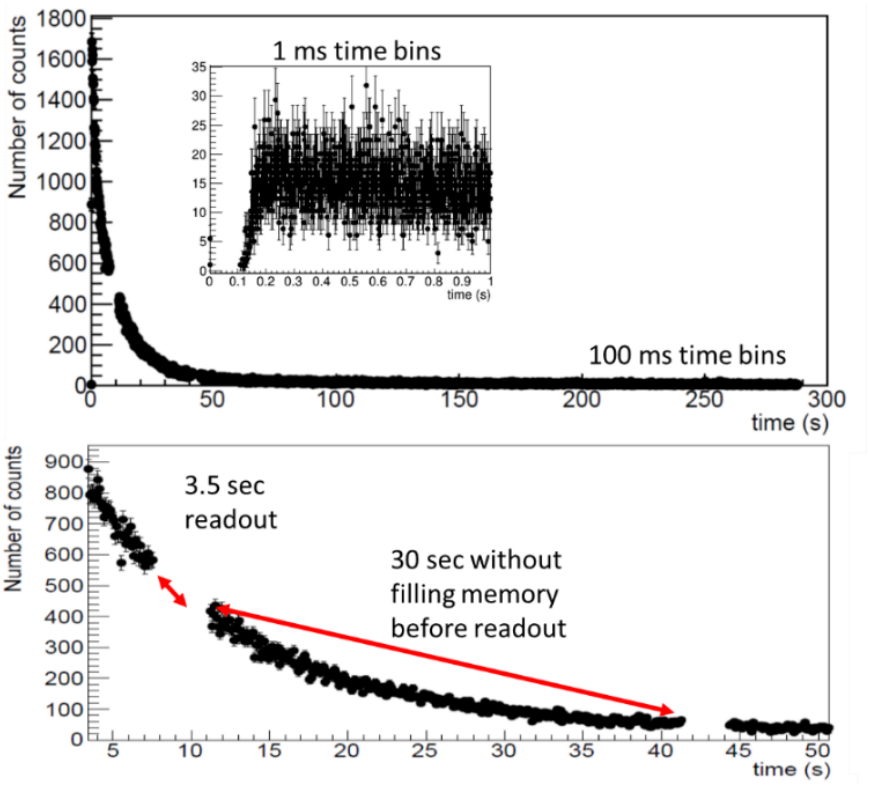

Figure 11. Results from getter detector in the OMEGA ride-along experiment. The decay curve from shot 96188 is shown with background rates reaching about 18,000 events per second. There were fewer readout "gaps" than with the turbopump detector, but still two in the time data was being collected.

1.6. Exploding Wire Experiment

To measure the fraction of the product nuclei trapped and detected in ICF implosions, an "exploding wire" experiment was designed, in which the "exploding wire" was a foil thinly coated with some radioactive material, similar to that in an actual ICF experiment (see Table

2). Copper and fluorine were chosen as possible target materials because they could be activated via $^{65}Cu(d,p)^{66}Cu$ and $^{19}F(d,p)^{20}F$ by a deuteron beam from a particle accelerator, producing ^{66}Cu and ^{20}F, which beta decay with 5.12 minute and 11.07 second half-lives, respectively. In the experiment, natural copper was electroplated onto a tungsten foil, or Teflon tape containing fluorine was wrapped around the tungsten foil. The target was irradiated by the particle accelerator at SUNY Geneseo, and a large current pulse through the tungsten rapidly heated the "exploding wire", vaporizing the radioactive target material so it expanded outward in a gas. The turbopump and getter trap and detector systems were attached to the test vacuum chamber in ports adjacent to the beam line, as shown in Figure 12, to trap and detect the expanding reaction products.

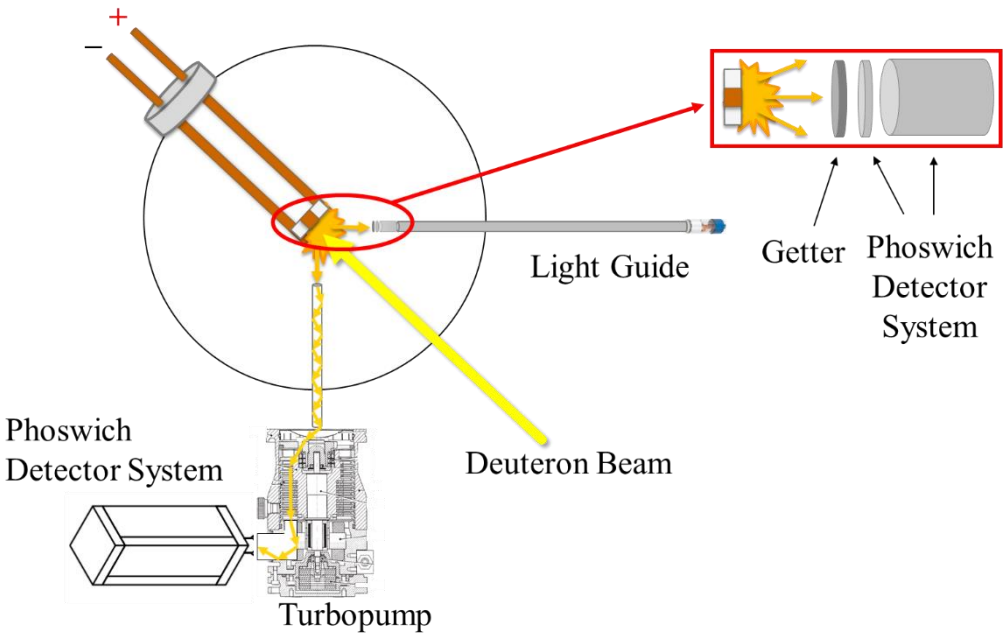

Figure 12. Schematic diagram of exploding wire experiment. The deuteron beam strikes the copper or fluorine target material, producing either ^{66}Cu or ^{20}F. A large current pulse through the tungsten vaporizes the target material, causing the radioactive isotopes to expand outward in a gas, simulating the ICF gas behavior. The turbopump and getter systems trap and detect the expanding reaction products.

Chapter 2

THEORY

2.1. Introduction

Since the goal of the experiment was to produce an ICF-like expanding gas, the material for the exploding wire needed to yield reaction products with the same characteristics as those from the reactions in Table 1. This chapter evaluates several considered materials and possible activation methods and discusses the properties of radioactive nuclei that were used to identify the trapped reaction products.

2.2. Exploding Wire Material

The reaction products from Table 1, ^{6}He, ^{8}Li, ^{12}B, ^{15}C, and ^{16}N, are each radioactive and beta decay with half-lives ranging from 20.2 ms to 7.13 s. The predicted yields, using ICF, of the most prolific of these reactions were nearing or exceeding 10^{6} reaction product nuclei. These short half-lives, high yields, and beta decays were the sought-after characteristics for the exploding wire material. A chemically reactive reaction product which would combine with a getter foil was also desired for the getter system, but not necessary for the turbopump system, which requires the gas to be relatively inert in order to not stick to the collection tube. Additionally, for the best results with the phoswich detectors, an endpoint energy of at least 1 MeV was required for the beta decays. The decay properties of possible reaction products are shown in Table 3, and their predicted yields, using either the particle accelerator or neutron howitzer at SUNY Geneseo, are shown in Table 4. Both tables show ^{64}Cu despite its long half-life because it is produced along with ^{66}Cu, as natural copper contains both stable isotopes, ^{63}Cu and ^{65}Cu.

The possible reactions to reach these products are also listed in Table 4, and involve striking the stable isotopes of the elements with protons or neutrons. This can be done directly with deuterons from the particle accelerator or with neutrons from the neutron howitzer. Other possible reactions involve neutrons produced by deuteron interactions, using the ^{2}H(d,n) reaction. The yields for neutron howitzer reactions assumed that the PuBe source had a

typical neutron yield of 10^7 neutrons per second, and that the neutrons radiated isotropically from the source and cooled to room temperature before reaching the target foil 15.2 cm away. The yields for the accelerator reactions assumed that the beam current was 10 nA with 3 MeV deuterons. The targets for both methods were assumed to have an area of 1 cm^2 and a thickness of 0.1 mm.

Table 3. Decay properties of ^{16}N, ^{20}F, ^{64}Cu, and ^{66}Cu nuclei. The beta and gamma decays are shown for each of the proposed reaction products, along with the endpoint energies for the beta decay spectrums. Table taken from Ref. [18].

	^{16}N	**^{20}F**	**^{64}Cu**	**^{66}Cu**
Half-life ($t_{1/2}$)	7.13 sec	11.07 sec	12.701 hr	5.120 min
Decay mode	β- (66.2%) Endpoint 4289.2 keV Average 1941.7 keV β- (28.0%) Endpoint 10419.1 keV Average 4979.8 keV	β- (99.99%) Endpoint 5390.86 keV Average 2481.5 keV	β+ (61.5%) Endpoint 653.0 keV Average 278.2 keV β- (38.5%) Endpoint 579.4 keV Average 190.7 keV	β- (9.01%) Endpoint 1601.7 keV Average 628.1 keV β- (90.77%) Endpoint 2640.9 keV Average 1112.1 keV
Gamma rays	6128.6 keV 7115.2 keV	1633.6 keV	511 keV 1345.8 keV	1039.2 keV

The predicted yields approach maximum values since the radioactive product nuclei decay as they are being produced. The decay rate starts out small, so the number of reaction products increases, but eventually the decay rate "catches up" to the reaction rate, leading to the maximum yield. This maximum yield is found by dividing the reaction rate by the reaction product's decay constant. The nuclear reaction rate is proportional to the flux of incident particles, the number density of target particles, and the active area and thickness of the target, with the nuclear cross section being the constant of proportionality. Mathematically, this is all represented by the general yield formula

$$N_{yield} = \frac{\sigma F N A t}{\lambda}, \tag{2.1}$$

where σ is the nuclear cross section, F is the flux of incident particles, N is the target number density, A is the area of the beam spot or target, t is the target thickness, and λ is the decay constant.

For the howitzer yields, the PuBe neutrons can potentially interact in the full volume of the target foil, so

$$N_{yield} = \frac{\sigma F N V_{foil}}{\lambda}, \tag{2.2}$$

where $V_{foil} = At$. For the accelerator yields, the total number of deuterons striking the target is determined by dividing the beam current, I, by the charge of an individual deuteron, e. This gives

$$N_{yield} = \frac{\sigma \frac{I}{e} N t}{\lambda}, \tag{2.3}$$

where $\frac{I}{e} = FA$. For the reactions caused by accelerator dd neutrons, the total number of neutrons is first predicted using

$$N_n = \sigma_{dd} \frac{I}{e} N t, \tag{2.4}$$

where σ_{dd} is the ^{2}H(d,n) cross section. Then the total yield is predicted using

$$N_{yield} = \frac{\sigma N_n N t}{\lambda}, \tag{2.5}$$

where $N_n = FA$.

One problem with the estimated yields was that the cross section for each reaction was not varied with depth as the neutrons or deuterons penetrated into the target foil. For example, the incident deuterons would lose energy as they passed through the material, giving a different cross section for each energy. Rather than integrating over the different cross sections based on the energies of deuterons interacting at different depths in the target, an average cross section was used. Another problem with the estimates was that the beam currents and energies were different for the actual experiment. The beam current was measured once to be 36.2 nA and the energy to be 1.514 MeV, rather than the assumed 10 nA and 3 MeV. Despite the uncertainties associated with these rough estimates, the predicted yields could still be used to choose a target material for the experiment.

Because the half-life of ^{66}Cu is relatively long, it had the highest predicted yield using the particle accelerator, making it the best choice for an initial experiment. Furthermore, copper is very sticky and would make a good candidate for the getter system. The ^{20}F yield from the particle accelerator was an order of magnitude lower but its half-life is closer to those of the reaction products in Table 1, making it the second best choice for the exploding wire material. Teflon tape, which would be used as the target material containing fluorine, also pyrolyzes into relatively inert molecules, making fluorine a good candidate for the turbopump system. Lastly, the ^{16}N yield was much lower than the best cases for the others, so it was not considered for the experiment. The direct deuteron (d,p) stripping reaction was chosen as the best method to activate the target materials to produce ^{66}Cu and ^{20}F.

Table 4. Predicted yields for possible reactions. Rough estimates are given for the maximum product yield for each reaction, assuming infinite irradiation time. The accelerator calculations assume a 10 nA beam current and 3 MeV deuterons. Neutron howitzer calculations assume 10^7 n/s PuBe source a distance of 15.2 cm from the target, with all neutrons moderated to room temperature and no absorption. All targets are assumed to be 1 cm^2 by 0.1 mm thick. Table taken from Ref. [18].

Reaction	Target	Source	Max. Yield
^{63}Cu(n,γ)^{64}Cu	Electroplated	Neutron howitzer	6.7×10^5
	Electroplated	Accelerator dd neutrons	7.8×10^5
^{65}Cu(n,γ)^{66}Cu	Electroplated	Neutron howitzer	2.7×10^5
	Electroplated	Accelerator dd neutrons	1.1×10^7
^{63}Cu(d,p)^{64}Cu	Electroplated	Accelerator d	1.5×10^9
^{65}Cu(d,p)^{66}Cu	Electroplated	Accelerator d	1.4×10^8
^{19}F(n,γ)^{20}F	Teflon coating	Neutron howitzer	0.3
	Teflon coating	Accelerator dd neutrons	2.4
^{19}F(n,α)^{16}N	Teflon coating	Accelerator dd neutrons	3300
^{19}F(d,p)^{20}F	Teflon coating	Accelerator d	2.3×10^7

2.3. Radioactive Isotopes

After the radioactive reaction products were trapped, their beta decays were detected. For copper, the rate of ^{66}Cu decays decreased over time, yielding a "decay curve", whereas the number of daughter nuclei ^{66}Zn increased over time, yielding a "growth curve". For fluorine, the rate of ^{20}Ne decays decreased over time and the number of its daughter nuclei ^{20}Ne increased over time. The half-lives of the detected reaction products could be determined by fitting decay or growth curves to the data, and then the reaction products could be identified

by their half-lives. This could determine whether or not the radioactive target material in the expanding gas was successfully trapped and detected.

The predicted decay curve is found by considering the rate at which the radioactive material decreases. This rate is proportional to the number of radioactive nuclei at a given time. Expressed in mathematical terms, if there are N radioactive nuclei, then

$$-\frac{dN}{dt} \propto N(t), \tag{2.6}$$

where $-\frac{dN}{dt}$ is the decay rate. The constant of proportionality is called the decay constant λ, giving the following differential equation:

$$\frac{dN}{dt} = -\lambda N. \tag{2.7}$$

The differential equation can be solved to give

$$N(t) = N_0 e^{-\lambda t}, \tag{2.8}$$

where N_0 is the initial number of radioactive nuclei at time $t = 0$. This equation represents the number of radioactive nuclei N at a time t; specifically, it shows how the number decreases exponentially over time. The half-life of a radioactive material, denoted by $t_{\frac{1}{2}}$, is simply the time it takes for half of the material to decay. The half-life can be found in terms of the decay constant by considering the condition

$$N\left(t_{\frac{1}{2}}\right) = \frac{N_0}{2} = N_0 e^{-\lambda t_{\frac{1}{2}}}, \tag{2.9}$$

so that

$$t_{\frac{1}{2}} = \frac{\ln(2)}{\lambda}. \tag{2.10}$$

In the exploding wire experiment, the detectors will measure the rate of decays. That is, they will measure the number of decays in a certain time period. This can be represented by taking the derivative of Eq. (2.8) with respect to time, giving

$$R(t) = -\frac{dN}{dt} = \lambda N_0 e^{-\lambda t} = R_0 e^{-\lambda t}, \tag{2.11}$$

where $R_0 = \lambda N_0$. The detectors will also inevitably measure some background radiation, which can be accounted for by adding a constant B to Eq. (2.11), giving

$$R(t) = R_0 e^{-\lambda t} + B, \tag{2.12}$$

the decay rate of radioactive nuclei as a function of time with constant background, also known as the decay curve.

The growth curve of any radioactive isotope's daughter nuclei is found by adding up the total number of decays over time. Mathematically, this is done by integrating Eq. (2.12) with respect to time. As the radioactive nuclei decay more rapidly near the beginning, the daughter nuclei increase more rapidly near the beginning. Eq. (2.12) is integrated to give

$$\int R(t)dt = -N_0 e^{-\lambda t} + Bt + C, \tag{2.13}$$

where the constant $C = N_0$ when considering the initial condition that $\int R(t)dt = 0$ when $t = 0$. Thus the growth curve with constant background is given by

$$\int R(t)dt = N_0\left(1 - e^{-\lambda t}\right) + Bt. \tag{2.14}$$

Either the decay curve or growth curve can be fit to data from the exploding wire experiment. The decay constant λ can be determined and used to calculate the half-life, which can be used to identify the isotopes trapped by the turbopump or getter. The background rate can also be determined from both curves, and the initial reaction rate R_0 can be determined from the decay curve directly, and the total number of detected nuclei N_0 can be determined from the growth curve directly, with the relation $R_0 = \lambda N_0$. The total number of detected nuclei N_0 must be measured as the first step in determining the fraction of trapped and detected reaction products. The second step in determining this fraction would be measuring the total reaction product activation in the exploding wire experiment, rather than relying on the predicted yields from Table 4.

Chapter 3

EXPERIMENTAL APPARATUS

3.1. Introduction

The main goal of the exploding wire experiment was to simulate the trapping and detection of the expanding radioactive gas produced by an ICF implosion, and determine the fraction of product nuclei trapped and detected by the turbopump and getter systems. To do this, a test vacuum chamber was transported to SUNY Geneseo and attached to the downstream side of the 30R scattering chamber on the 1.7 MV tandem Pelletron Accelerator. The accelerator produced a beam of deuterons which entered the test chamber to strike a copper plated or Teflon wrapped tungsten ribbon suspended in the center of the test chamber by the exploding wire device. The beam was incident on the copper plated target for approximately 30 minutes to activate copper via $^{65}Cu(d,p)^{66}Cu$, or for the Teflon wrapped target for about 90 seconds to activate fluorine via $^{19}F(d,p)^{20}F$. Unfortunately, only copper was evaporated in the experiments to date. This was done with a large current pulse through the tungsten which rapidly heated and vaporized the copper, resulting in a radioactive expanding gas. Once the radioactive expanding gas was produced, attempts were made to trap and detect the product nuclei with the turbopump and getter systems, which were attached to the test chamber on ports adjacent to the beam port, as shown in Figure 13.

In addition to the main exploding wire experiment, several other experiments were conducted. The first involved activating copper with a neutron howitzer to determine whether or not the turbopump and getter detectors could successfully detect ^{66}Cu. Radioactive fluorine was also produced using the particle accelerator and detected in situ with the getter detector, though it was never evaporated. A second set of experiments was carried out with a remote controlled rotating shield, which was designed to determine whether or not any copper stuck to the tungsten ribbon after the "explosion". Lastly, experiments were performed with a separate detector with known efficiency to measure the total number of ^{66}Cu nuclei produced by the accelerator.

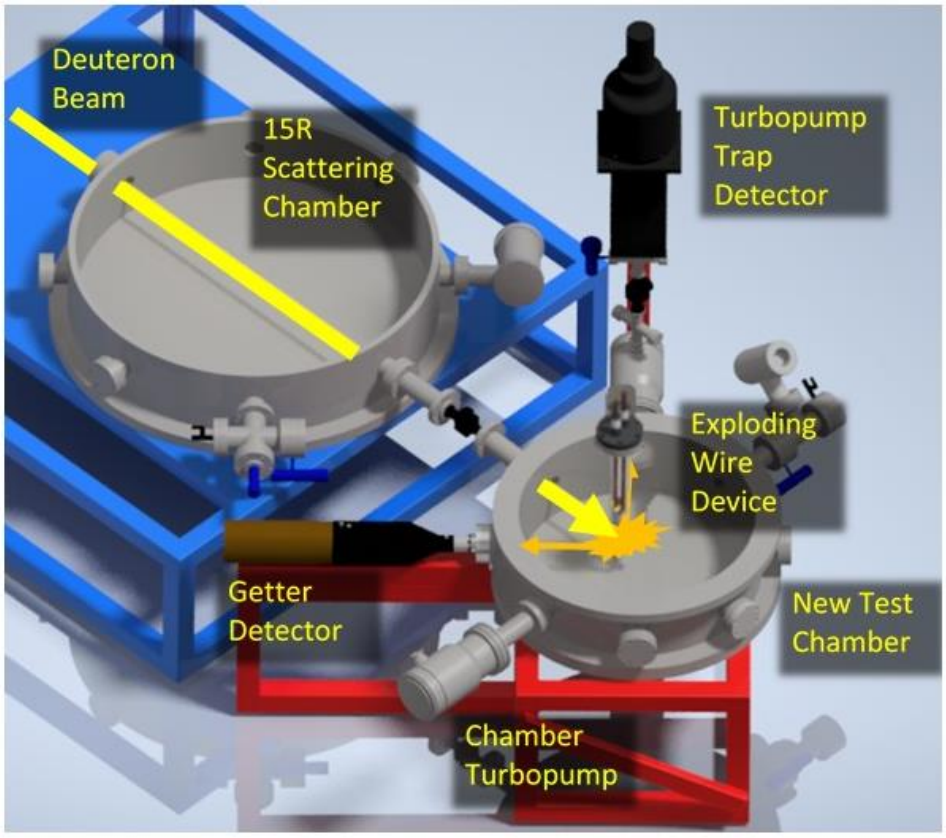

Figure 13. Three-dimensional diagram of exploding wire experiment. The deuteron beam passed through the scattering chamber into the test chamber, which was evacuated by the chamber turbopump. The beam struck the tungsten ribbon suspended by the exploding wire device, activating the coating material. Then a large current pulse passed through the tungsten, evaporating the radioactive material so it could be trapped and detected by the getter and turbopump systems.

3.2. Test Chamber

The test chamber was a stainless steel cylindrical vacuum chamber with a diameter of 50.8 cm (20 in.) and height of 15.24 cm (6 in.). Around its perimeter were eight 2.75 in. conflat ports, and in a line across the top of the chamber lid were two 2.75 in. and three 1.33 in. conflat ports. The test chamber was attached to the 30R scattering chamber on SUNY Geneseo's 1.7 MV tandem Pelletron accelerator via one of the ports around its perimeter. Between the two chambers was a pneumatic gate valve. This valve could isolate the test chamber from the rest of the accelerator's vacuum system.

Attached to the other seven ports circling the test chamber were the trap and detector systems, viewing windows, the test chamber's turbopump, pressure gauges, back-to-air valve, and a residual gas analyzer, as shown in Figure 14. The getter system was attached to the beam-right port and the turbopump system was attached to the beam-left port. Both trap and detector systems will be discussed in later sections. Two 2.75 in. conflat viewing windows were attached to the opposing ports next to each of the trap and detector systems.

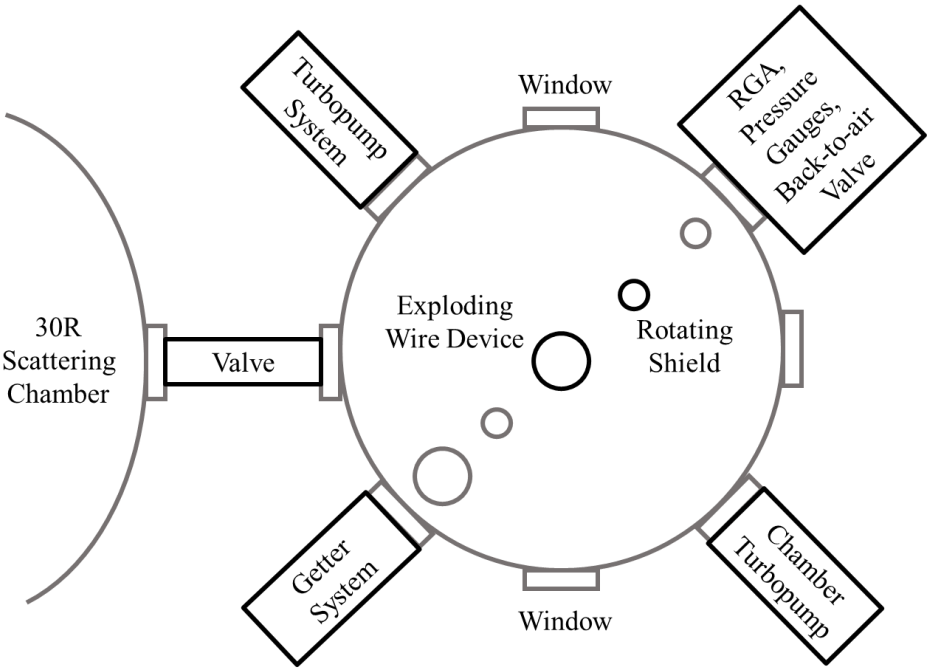

Figure 14. Top view of exploding wire experiment apparatus. The beam enters the test chamber from the 30R scattering chamber when the pneumatic gate valve is open. The exploding wire device is placed in the central top port with the rotating shield behind it, with respect to the getter system. The getter system is attached to the beam-right port and the turbopump system is attached to the beam-left port. Viewing windows are placed on either side of the test chamber next to each trap and detector system, with the chamber turbopump and various pressure gauges next to them.

The test chamber turbopump was a Pfeiffer Balzers TPH-062 Turbopump with a TCP-121 controller, backed by an Alcatel Pascal 2005 SD fore pump. When the fore pump evacuated the chamber to about 20 mTorr, the turbopump was turned on and used to evacuate the chamber to about 5×10^{-6} Torr, a pressure low enough to open the test chamber's gate valve

to the accelerator's vacuum system. After coming to equilibrium with the accelerator's vacuum system, the pressure stayed in the low 10^{-6} Torr range.

The pressure gauges, back-to-air valve, and residual gas analyzer were attached with standard 2.75 in. vacuum Tees to the test chamber port. An SRS RGA100 residual gas analyzer was used to determine whether residual chamber pressure was due to air or water. A Granville-Phillips Convectron pressure gauge was used with a GP 275 controller to measure the pressure down to about 10^{-3} Torr, and a Duniway 1-100-K ion gauge was used with an SRS IGC-100 controller to measure the pressures below about 10^{-4} Torr. The back-to-air valve was connected to a nitrogen gas cylinder to fill the test chamber with dry nitrogen to avoid moisture from the air.

Attached to the port opposite the beam port was an insulated 2.75 in. conflat flange which served as a Faraday cup to measure the beam current reaching the back of the test chamber. The current was measured using an electrometer to be 36.2 nA by the Faraday cup and the energy of the deuterons was measured by to be 1.514 MeV in the 30R scattering chamber before reaching the test chamber. Both measurements were taken hours before the first copper-plated tungsten ribbon was successfully activated.

The test chamber lid was oriented with the five conflat ports in line with the getter system. The exploding wire device was inserted into the central 2.75 in. conflat port, and the rotating shield rotation feedthrough was inserted into one of the adjacent 1.33 in. conflat ports, as shown in Figure 14.

3.3. Exploding Wire Device

The exploding wire device was designed and constructed by a team of SUNY Geneseo students. The device originally consisted of a 2.75 in. conflat electrical feedthrough with four copper rods penetrating through it in a square pattern, as shown in Figure 15. For initial testing, the flange was attached to a different vacuum chamber at SUNY Geneseo and two tungsten ribbons were each bolted across two of the four copper rods. The ends of the copper rods outside the chamber were attached to a battery that provided the large current pulses through the tungsten.

The four rods were originally designed to allow two tungsten ribbons to be tested at the same time, rather than just one. For the main experiment, however, they served the purpose of being able to easily change the direction of the tungsten ribbon, so that it could face either the getter system or the turbopump system. Two larger copper rod extenders, also shown in Figure 15, were attached with set screws to two of the original four rods so the tungsten ribbon could be suspended into the center of the vacuum chamber. The depth from the top of the test chamber's conflat flange to which the device was attached, to the center of the test chamber was 14.1 cm. When the direction of the tungsten ribbon needed to be switched to face a different trap and detector system, the two larger copper rod extenders were detached, rotated 90 degrees, and reattached to the other two smaller copper rods.

Figure 15. Exploding wire device with tungsten ribbon target. Four copper rods pass through the conflat electrical feedthrough with two larger copper extenders able to hold the tungsten ribbon in the center of the test chamber. The tungsten ribbon may face either the getter system or the turbopump system by detaching the copper extenders, rotating them 90 degrees, and reattaching them to the other two copper rods.

The tungsten ribbons used for the experiment were approximately 0.05 mm thick and were cut into approximately 6.5 mm by 12.5 mm strips. The primary coating material, copper, was

electroplated onto the tungsten ribbons out of a saturated copper sulfate solution. Another team of SUNY Geneseo students was responsible for electroplating the targets. The general procedure involved first preparing the electrodes by roughening them with 400 grit emery cloth and then cleaning them with distilled vinegar and DI water. Next 200 g of $CuSO_4$ were stirred into 800 mL of distilled water, and copper and tungsten electrodes were suspended into the solution with alligator clips. An approximate 1 A current was allowed to pass between the electrodes, and the voltage increased from about 3.3 V to 3.9 V in the typical electroplating process.

The copper was electroplated with various thicknesses and covered different areas of the tungsten ribbons. Most experiments involved copper thicknesses of 11 μm and 25 μm. The 25 μm layer was electroplated across the full tungsten ribbon on both sides, and the 11 μm layer was electroplated only in an approximate 6.5 mm square in the center of one side of the ribbon. Other experiments involving fluorine used Teflon tape, which was wrapped around the tungsten ribbon.

3.4. Control Systems

During the exploding wire experiment, no one was allowed near the target chamber or beamline due to the neutron radiation produced by the deuterons striking accelerator components. For this reason, the valve between the two vacuum chambers, the relay that allowed current to heat the tungsten ribbon, and the rotating shield all had to be controlled remotely from a safe distance. There were also two more pneumatic valves that were part of the turbopump trap discussed later. The "control room" was located in the hall directly outside the accelerator lab and contained the computer used for controlling the valves, relay, and shield, and for data acquisition, which is described in the next section.

3.4.1. Valves

The gate valve between the test chamber and the 30R scattering chamber was a VAT gate valve and the turbopump system valves were VAT inline valves. All three were opened and closed by Tailonz pneumatic switches. The pneumatic switches were attached to an air compressor operating at approximately 100 psi via 3.9 mm diameter plastic tubing and required 12 V to open and close the valves. A control box, implementing the circuit shown in

Figure 16, was designed to open and close the valves manually using switches or remotely using computer controls. When the manual switches were closed the valves were opened, and when the manual switches were open the valves were closed. The valves could also be controlled using MOSFETs which were switched on and off using the GP10 pins of an Arduino microcontroller. The relay system responsible for allowing current to heat the tungsten ribbon is shown on the right side of the diagram and could also be switched manually or automatically like the valves.

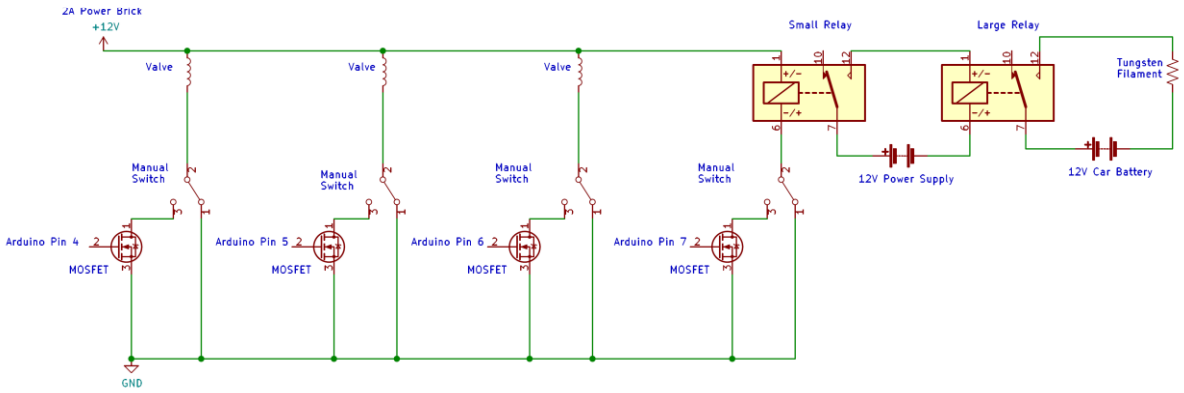

Figure 16. Schematic diagram of circuit used to control the valves and battery. The circuit allows for manual control of the valves using external switches in addition to remote control using MOSFET switches and an Arduino web server. Two relays were used since the original small relay used to supply power to the valve switches was unable to also allow the 12 V car battery to heat the tungsten ribbon.

3.4.2. Relays

The relay responsible for allowing current to pass through the tungsten ribbon would have used the same 12 V power supply that powered the pneumatic switches, but this power supply could not provide enough current. Instead, a second relay was used in a circuit with the first relay with an additional 12 V power supply, as shown in Figure 16. This second high current relay closed the circuit between the 12 V car battery and the tungsten ribbon. The battery supplied an approximate 100 A current pulse through the tungsten for about 10 seconds to evaporate the electroplated copper or Teflon. The heated tungsten ribbon is shown through one of the vacuum windows in Figure 17, with the end of the collection tube from the turbopump system also visible.

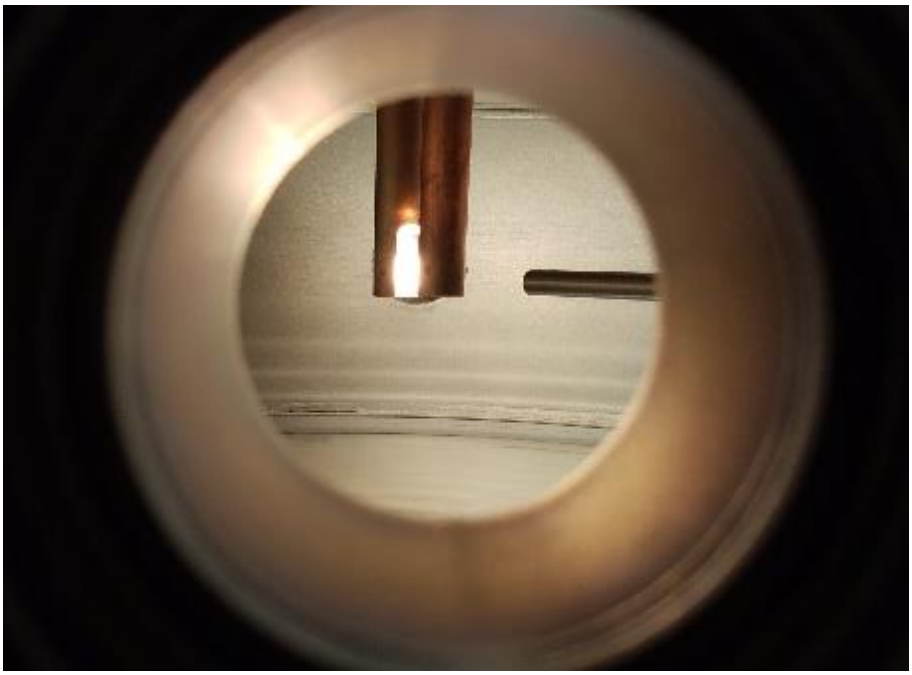

Figure 17. Heated tungsten ribbon inside the test chamber. The tungsten ribbon was heated with a 12 V car battery providing an approximate 100 A current pulse lasting 10 seconds. Viewing the target through one of the chamber windows, the end of the turbopump system's collection tube is also visible.

The valves and relays were controlled remotely by connecting the control box with a cable to an external MOSFET board, which was controlled by an Arduino Mega. The Arduino served a webpage using an ethernet shield with the same private network used for data acquisition.

3.4.3. Shield

The Arduino was also used to control the position of the rotating shield. The shield consisted of an "L" shaped strip of 0.92 mm thick aluminum attached to a steel rod extending from a rotary feedthrough, which was attached to one of the 1.33 in. ports next to the exploding wire device. The 14.1 cm by 4.2 cm "L" shaped shield cleared the exploding wire device by approximately 1 cm when rotating. The shield's default position was set to block the test chamber's turbopump port to prevent any copper from depositing on the turbopump's blades. The Arduino was able to rotate the shield 120 degrees to rest between the tungsten ribbon and the getter detector. The original motivation was to prevent the getter detector from detecting any copper left on the ribbon after evaporating by moving the shield in between the ribbon and detector. However, most beta particles from any residual copper

would have sufficient energy to pass through the thin aluminum shield. Instead of moving the shield between the detector and target after the explosion, the shield was moved into position before the explosion to "catch" the evaporated copper, blocking any from hitting and sticking to the getter. Then the shield was rotated back to the default position far from the getter detector, so any residual copper on the target could be isolated and measured directly by the getter detector. To rotate the shield, a servo motor was attached to the top of the feedthrough with 3-D printed plastic parts, as shown in Figure 18. The motor was attached to one of the PWM pins on the Arduino Mega and programmed to move between the two positions.

Figure 18. Rotating shield with servo motor. The 0.92 mm thick aluminum shield formed a 14.1 cm by 4.2 cm "L" shape. The shield was attached to the test chamber lid with a rotary feedthrough, and a servo motor was mounted with 3-D printed plastic parts to rotate the shield. The shield blocked the inside of the test chamber's turbopump port in its default position, and could rotate 120 degrees to rest between the getter detector and the target.

3.5. Detectors

Once the test chamber was evacuated, the accelerator valve was opened, and the copper or Teflon was irradiated and evaporated, the ^{66}Cu or ^{20}F would expand outward in a gas toward the getter or turbopump systems to be trapped and detected. The trap and detector designs for each system will be described in the final sections of this chapter, but the general purpose and assembly of the phoswich detectors will first be discussed.

3.5.1. Phoswich Detectors

The phoswich detectors consisted of two plastic scintillator detectors sandwiched together. These scintillator detectors emit flashes of light when charged particles pass through and were optically coupled to a photomultiplier tube (PMT) to convert the light to current pulses. The heights of these pulses are proportional to the light emitted, and the light emitted is proportional to the energy lost by the particle passing through the scintillator. For this reason, particles can often be identified by the pulse heights. For example, monoenergetic particles will all have pulse heights unique to their energy and can be distinguished from particles with different energies.

The two scintillators differed in that one was made of a "thin fast" plastic and the other was made of a "thick slow" plastic, with the speed referring to how quickly the light is emitted. These are referred to as the "dE" and "E" detectors, respectively, since only a small amount of energy is lost in the first, and most of the particle's energy is lost in the second. The typical assembly of a phoswich detector is shown in Figure 19.

Each scintillator gives a unique pulse shape because of the plastic used, and the differences can help distinguish beta particles from possible background gamma radiation. This is because when beta particles pass through the detector head-on, they lose some energy in the dE detector and more energy in the E detector, triggering both detectors and giving two unique pulses. Photons, however, do not constantly lose energy in the same way as they pass through matter; they either interact or go undetected, giving only one pulse as they pass through the detectors. Examples of possible pulse shapes viewed on a Tektronix TDS 2024B oscilloscope are shown in Figure 20, with the dE pulse on the left, the E pulse in the middle,

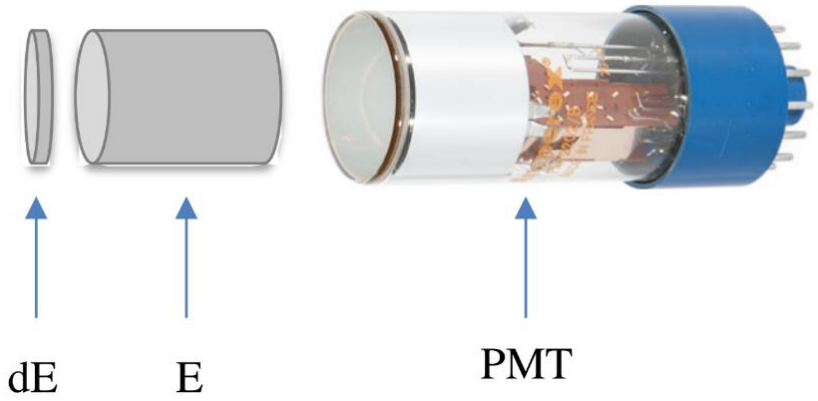

Figure 19. Typical phoswich detector assembly. The detector consists of two plastic scintillators, a thin fast plastic (dE) and a thick slow plastic (E). The detectors emit light when charged particles pass through, which is converted to a current pulse by a PMT. The speed of each scintillator refers to how fast the light is emitted, so each detector gives a unique pulse shape that can be used to identify beta particles.

and the combined dE-E pulse on the right. A ^{207}Bi source, which emits a spectrum of beta particles as well as approximately 1 MeV and 0.5 MeV monoenergetic beta particles, was used to produce the pulses of Figure 20. The combined pulse shapes are considered to be caused by beta particles, while the individual dE and E pulses are considered to be caused by background gamma radiation. Of course, the dE pulses could also be caused by low energy beta particles stopping before reaching the E detector, and the E pulses could also be caused by beta particles reaching the detector from some other angle rather than head-on, though these scenarios are not as likely as background gamma radiation events.

3.5.2. Electronics

To distinguish the "good" beta events from possible background radiation, points from each pulse were plotted on a 2-D histogram with dE pulses on the vertical axis and E pulses on the horizontal axis, as shown in Figure 21. Each data point corresponded to the integral of a pulse, which was proportional to the pulse height and therefore the energy deposited by the particle, meaning the energies of particles could be measured. The dE-only pulses formed a band of points on the left-hand side of the plot and the E-only pulses formed a band of points across the bottom of the plot. These were primarily comprised of background events, while the combined pulses between the two bands made up the majority of "good" beta events. The

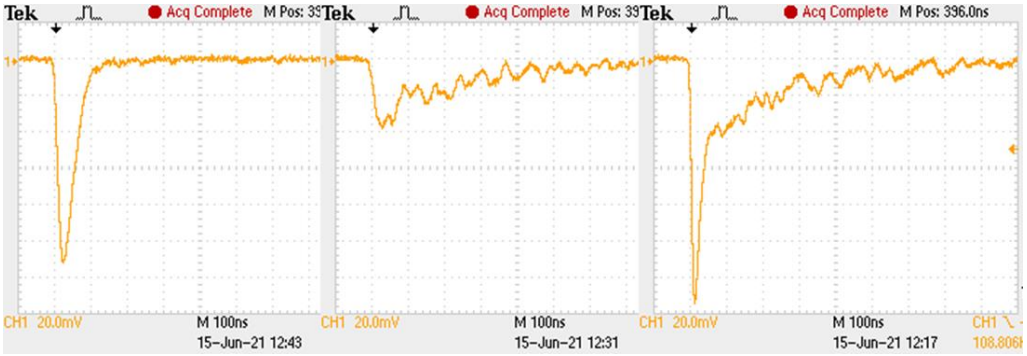

Figure 20. Possible pulse shapes from a phoswich detector. A ^{207}Bi source, emmitting a spectrum of beta particles as well as 1 MeV and 0.5 MeV monoenergetic beta particles, was used to produce the pulses, which were viewed on a Tektronix TDS 2024B oscilloscope. The left pulse was from the dE detector, the middle pulse was from the E detector, and the right pulse was from both detectors.

^{207}Bi source was used again with the getter detector to produce the 2-D histogram of Figure 21, with the 1 MeV monoenergetic beta particles showing up as a darker grouping of points between the dE and E bands. The ^{207}Bi source was frequently used to calibrate the detectors and electronics. Other points between the bands were from beta particles emitted at different energies and hitting at different angles, and the green box was used to select only the "good" beta events for data analysis.

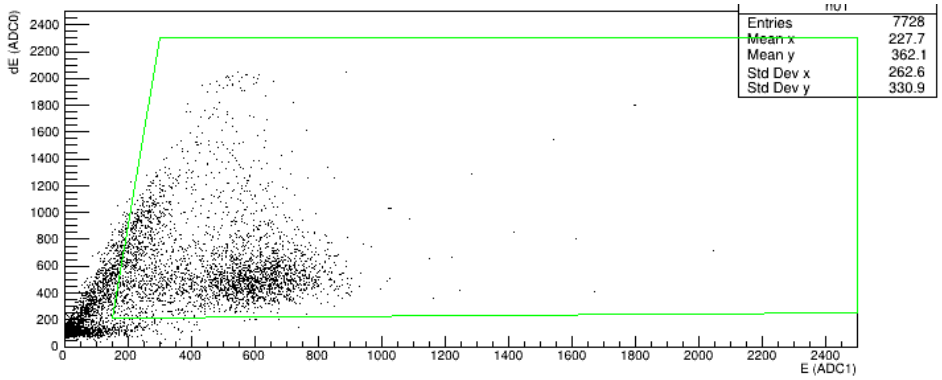

Figure 21. Two dimensional histogram of events detected from a ^{207}Bi source. Pulses from the dE detector are plotted on the vertical axis and pulses from the E detector are plotted on the horizontal axis. The channel numbers of each axis are uncalibrated, but proportional to the energy lost by each particle in the detectors. Individual pulses from each detector form two bands of points, and "good" beta events from both detectors fall between the bands. The 1 MeV monoenergetic particles are seen as a darker grouping of points, and the other points between the bands are comprised of beta particles emitted at different energies and striking at other angles.

NIM electronics were used to process the signals, and a FemtoDAQ acquisition system digitized the pulses coming from the detector's PMT. Conceptually, the electronics split the combined pulses into the separate dE and E components and recorded the integral of each pulse on the 2-D histogram. Pulses with only a dE or E component would be recorded as such without the need to separate the two components. The dE and E components were separated by sending the combined pulse through two gates. One gate allowed only the dE component to pass through and the other gate allowed only the E component to pass through. Each component was sent to the FemtoDAQ and digitized on the 2-D histogram. A combined dE and E pulse would be plotted with a dE and E component while an individual dE or E pulse would only be plotted with the corresponding component. A block diagram of the electronics responsible for separating the pulses is shown in Figure 22.

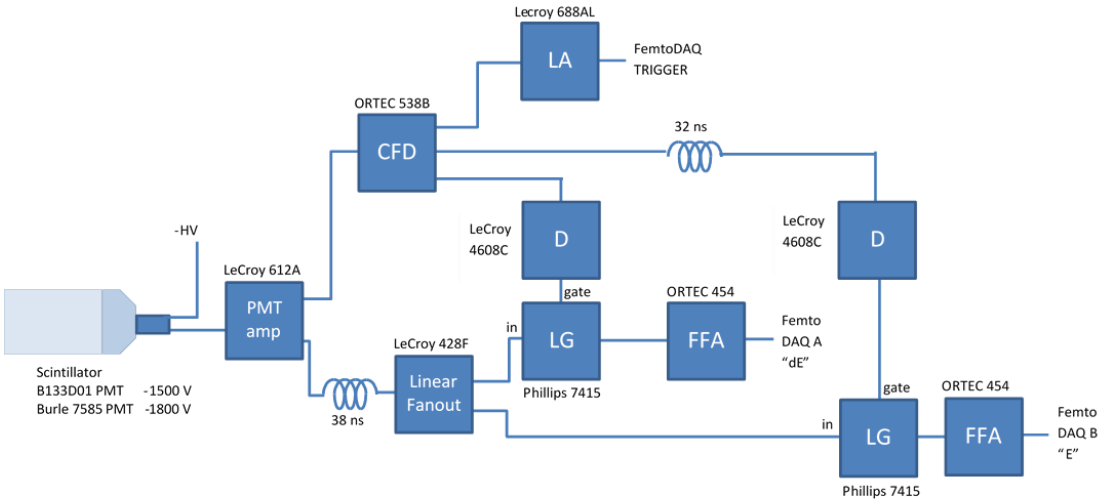

Figure 22. Block diagram of the electronics used to process pulses from the detector. A pulse is first amplified (PMT amp) and split (Linear Fanout), and then sent to two linear gates (LG) so the dE and E components can be separated. The linear gates are gated using logic pulses from the constant fraction discriminators (CFD) that are timed for the correct durations to select the dE and E components of the pulses. The CFD also triggers the FemtoDAQ to digitize the dE and E components. Lastly, the fast filter amplifier (FFA) integrates each pulse to digitize points proportional to the energies of detected particles.

3.6. Getter System

The getter trap and detector system consisted of the getter foil, a phoswich detector, a light guide, and a PMT, as shown in Figure 23. One possible idea proposed for an ICF experiment

would be to direct the plasma toward the getter foil using a high voltage, which was not tested in this series of experiments, since the ^{66}Cu or ^{20}F reaction products would not be ionized. The ^{66}Cu or ^{20}F nuclei would stick to the getter foil after evaporating off the tungsten ribbon, and then their beta decays would be detected by a phoswich detector system. The phoswich detector system included a light guide to transmit the light from the scintillator detectors to the PMT which was attached on the outside of the test chamber.

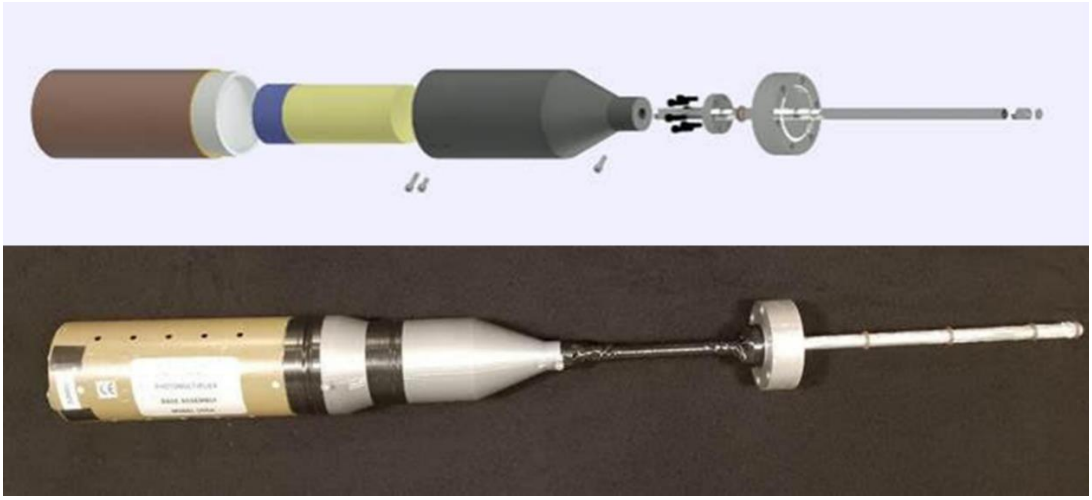

Figure 23. Getter trap and detector system. After evaporating the target material, the ^{66}Cu or ^{20}F nuclei stuck to the getter foil (right). The beta decays were then detected by the phoswich detector, which transmitted light through the light guide to the PMT for data analysis. A 3-D printed plastic cover was used to secure the light guide to the PMT, and a custom vacuum flange was designed to attach the assembly to the test chamber.

3.6.1. Getter Foil

The getter foil was made of 5.1 μm thick aluminum foil because it would reflect light emitted by the scintillators back toward the PMT, and copper would easily stick to it. Thin aluminum foil was used so the beta particles would lose very little energy when passing through it to reach the scintillator, however the thickness had to be balanced with the difficulty of folding the foil over the face of the detectors without tearing it. Any holes in the aluminum foil would allow light from the glowing tungsten ribbon to reach the PMT.

3.6.2. Phoswich Detector

The dE detector in the phoswich detector system was a fast EJ-212 cylindrical scintillator with a decay time of 2.4 ns [19], a thickness of 1 mm, and a diameter of 9.5 mm. The E

detector was a slow EJ-240 cylindrical scintillator with a decay time of 285 ns [19], a thickness of 15 mm, and a diameter of 10 mm. The two scintillators were optically coupled to each other using EJ-500 optical epoxy, and then the dE detector was optically coupled to one end of the light guide with the same epoxy. The sides of the scintillators were also wrapped with aluminum foil to reflect stray light back toward the light guide to the PMT.

3.6.3. Light Guide

The getter system used a glass optical fiber light guide which had a 10.1 mm diameter and 45.9 cm length. The lightguide was manufactured by Fiberoptics Technology Incorporated with a 0.66 numerical aperture and a 0.395±0.005 in. clad depth. The end opposite of the detectors was optically coupled to the PMT with EJ-550 optical silicone grease. A special 2.75 in. flange was made with a hole large enough for the light guide to loosely fit through. A #110 Viton O-ring was fit around the light guide and compressed against the outside of the custom flange to make a vacuum seal possible. Like the phoswich detector, the light guide was also wrapped in aluminum foil to reflect stray light toward the PMT. On the outside of the test chamber, light-tightness was ensured by wrapping the light guide with black electrical tape over the aluminum foil, and inside the test chamber, the light guide was made light-tight by wrapping the foil with Teflon tape, all the way up to but not covering the getter foil.

Prior to assembling the detector, various materials were tested for the light guide to see which transmitted the highest percentage of light to the PMT. Unfortunately, even the best light guide absorbed or lost most of the light emitted by the phoswich detector. Besides glass optical fiber, two other materials, acrylic and polycarbonate, were tested. They were cut, sanded, and polished to be close to the same dimensions as the glass light guide. The acrylic light guide was 0.91 cm in diameter and 46.0 cm in length, and the polycarbonate 0.90 cm in diameter and 46.0 cm in length.

The light guides were tested using the thin dE scintillator detector and a 1 μCi ^{241}Am source. This source emitted monoenergetic alpha particles at about 5 MeV, meaning all the PMT pulses had roughly the same pulse height. First, the dE detector was optically coupled directly to the PMT with the EJ-550 optical silicone grease, and the ^{241}Am source was placed as close as possible to it. This gave a pulse height proportional to the energy of the emitted

alpha particles, which was measured using a Spectech UCS 30 multichannel analyzer (MCA). Next, the dE detector was optically coupled to each light guide in sequence, the light guide was optically coupled to the PMT, and the ^{241}Am source was placed as close as possible to the detector. The energy the alpha particles deposited was the same, but the amount of light transmitted from the detector to the PMT was much less. The same measurement using the MCA was recorded. Finally, the same process was repeated after wrapping the light guide with aluminum foil, to reflect stray light back toward the PMT.

This test was performed for each of the three materials. However, it was difficult to achieve consistent results particularly when the light guide was wrapped with foil. Since optical grease was used rather than optical epoxy, the light guide could be easily bumped out of place, which often degraded the optical connection. Consistent results were more easily achieved without the foil because the connection could be easily observed. Careful measurements with foil were made only with the most promising light guide, the glass light guide, and the transmission bonus given by the foil, of about 31%, was used to estimate the "with foil" measurements for the acrylic and polycarbonate light guides. The results of the transmissions for each light guide are shown in Table 5.

Table 5. Light guide transmissions for different materials. Glass optical fiber, acrylic, and polycarbonate were all tested as possible light guide materials. Each was tested without aluminum foil, but the most promising glass light guide was tested with foil, and the effect of the foil was used to estimate the "with foil" cases for the other two materials, shown in red.

Light Guide	Length (cm)	Diameter (cm)	MCA Measured Transmission (Foil)	MCA Measured Transmission (No Foil)
Glass	45.9	1.01	42%	32%
Acrylic	46.0	0.91	29%	22%
Polycarbonate	46.0	0.90	0%	0%

3.6.4. Photomultiplier Tube

Two PMT models, a Photonis XP 2262 and a Burle 7585, were also tested for the getter system to see which worked best with the glass light guide. The 0.1 μCi ^{207}Bi source was used

with the getter detector both with and without the glass light guide for each PMT. Since a large fraction of the light was lost through the light guide, the pulses were smaller, and their shape was less obvious. The light guide pulses were "noisier" because of individual photons reaching the PMT, since the fraction of transmitted light was so low. As shown in Figure 24, the Burle 7585 PMT seemed to retain the original pulse shape better with the light guide, so it was the obvious choice for the experiment.

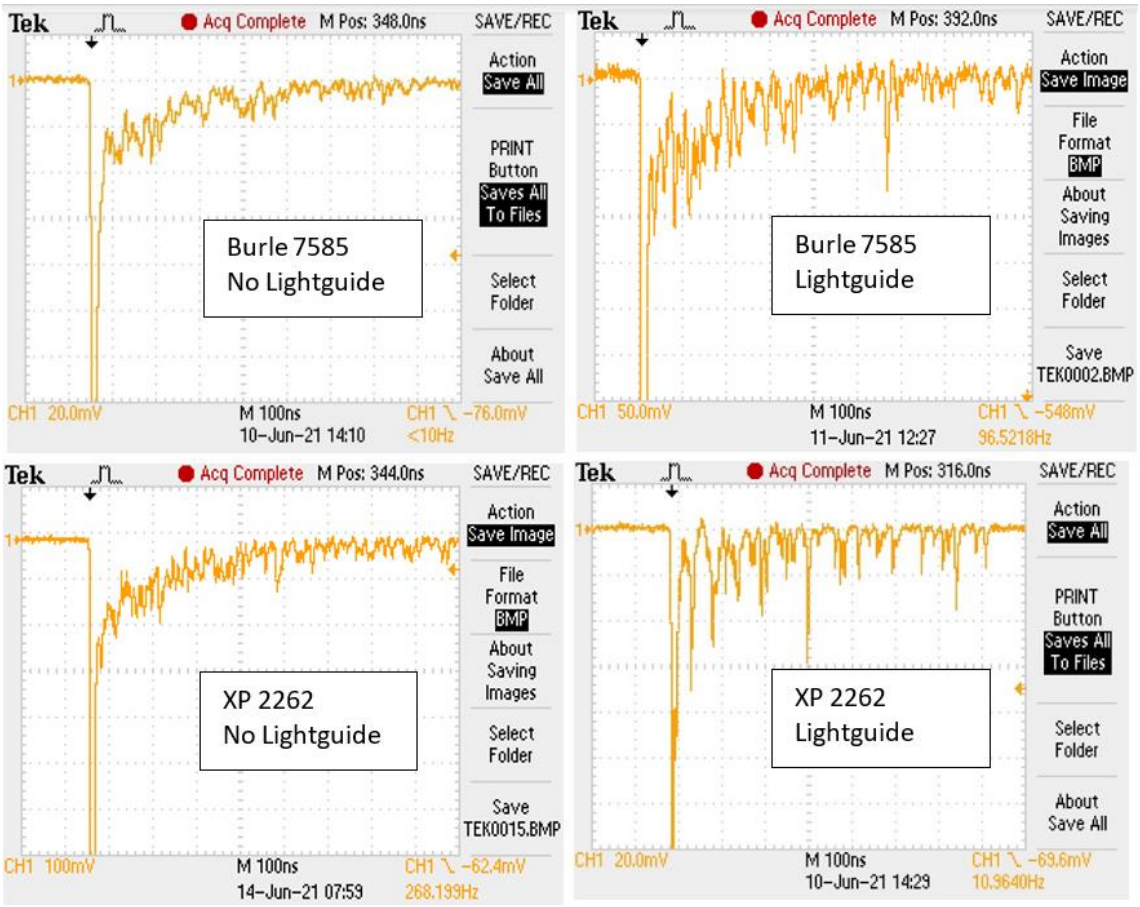

Figure 24. Light guide tests with Burle 7585 and Photonis XP 2262 PMTs. The ^{207}Bi source was used again with the getter detecter optically coupled to the glass light guide. The light guide was optically coupled to two different test PMTs, in sequence, to determine which best kept the combined shape of the dE and E pulses. The Burle 7585 PMT appeared to keep the shape better than the XP 2262 PMT.

3.7. Turbopump System

The turbopump system consisted of the collection tube, turbopump, pneumatic valves, and phoswich detector system, as shown in Figure 25. After adjusting the exploding wire device

to face the collection tube, the ^{66}Cu or ^{20}F nuclei would be evaporated off and some fraction would enter the tube. Then the atoms would travel down the collection tube and into the turbopump which would trap them inside the phoswich detector, which was attached to the turbopump exit port with a series of pneumatic valves. The decays would then be detected, and the light would be converted to current pulses by the PMT optically coupled to one of the faces of the detector.

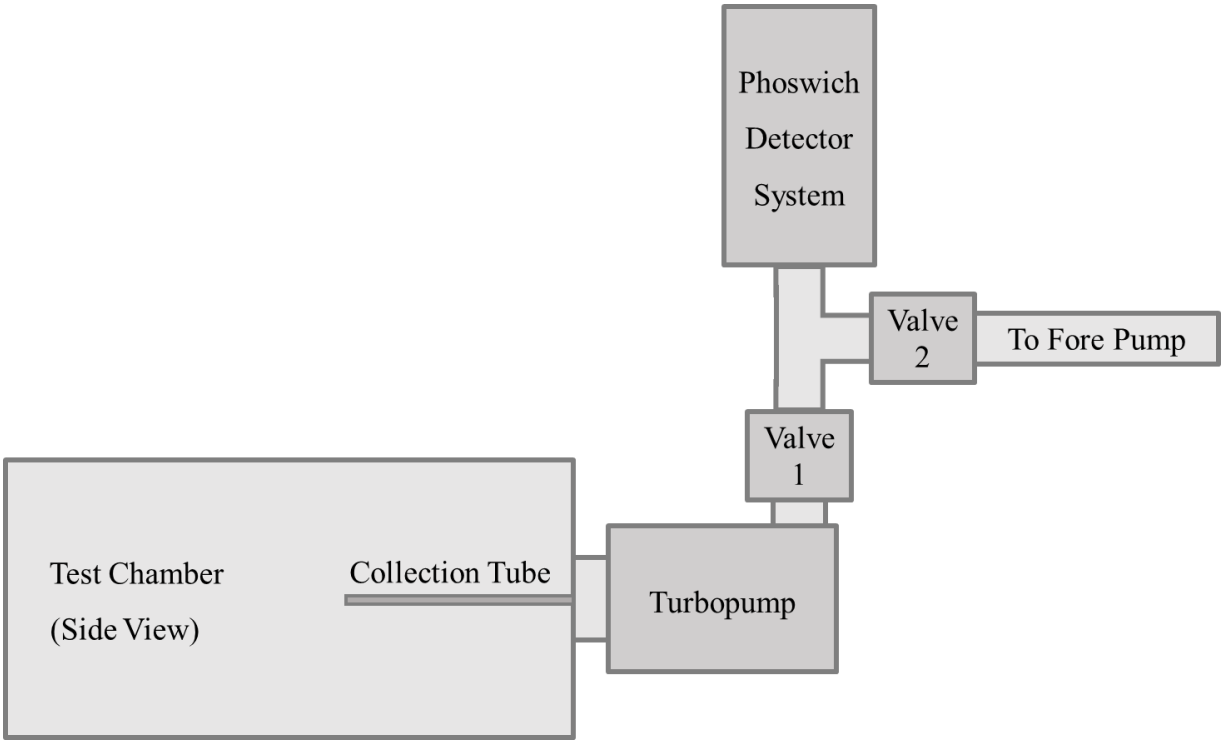

Figure 25. Turbopump trap and detector system. After evaporating the target material, the ^{66}Cu or ^{20}F would enter the collection tube. With Valve 1 open and Valve 2 closed, the turbopump would trap the ^{66}Cu or ^{20}F nuclei inside the phoswich detector system, where the beta decays would be detected.

3.7.1. Turbopump Trap

The collection tube was an aluminum tube 6.34 mm in diameter and 27.1 cm in length, extending into the chamber 18.1 cm from the center of a hollow aluminum cylinder that fit tightly into the turbopump's chamber port. The end of the collection tube was about 3 cm from the target suspended in the chamber. An Edwards EXT70H Turbopump was attached to the outside of the chamber port and used a BOC Edwards EXC120 controller. Attached to

the turbopump's outlet QF16 port were the two pneumatic valves mentioned earlier for switching between pumping with the fore pump and trapping the gas.

Both valves had one end attached to the phoswich detector system through the use of a QF16 vacuum Tee, as seen in Figure 25. The first valve, labeled Valve 1, was attached to the outlet of the turbopump, and the second valve, labeled Valve 2, was attached to the fore pump. In the experiment testing the turbopump system, the turbopump was powered on for the entire experiment, so Valves 1 and 2 were open to the fore pump until just before the target material was evaporated. Then valve 1 was allowed to stay open, Valve 2 was closed, and the ^{66}Cu or ^{20}F was evaporated. The ^{66}Cu or ^{20}F nuclei were able to pass through Valve 1 and the only path would lead to the phoswich detector system. After about 20 seconds, Valve 1 was closed and the beta decays of the trapped ^{66}Cu or ^{20}F nuclei were detected.

3.7.2. Phoswich Detector System

The phoswich detector for the turbopump system was built and tested in 2019 [14]. It used

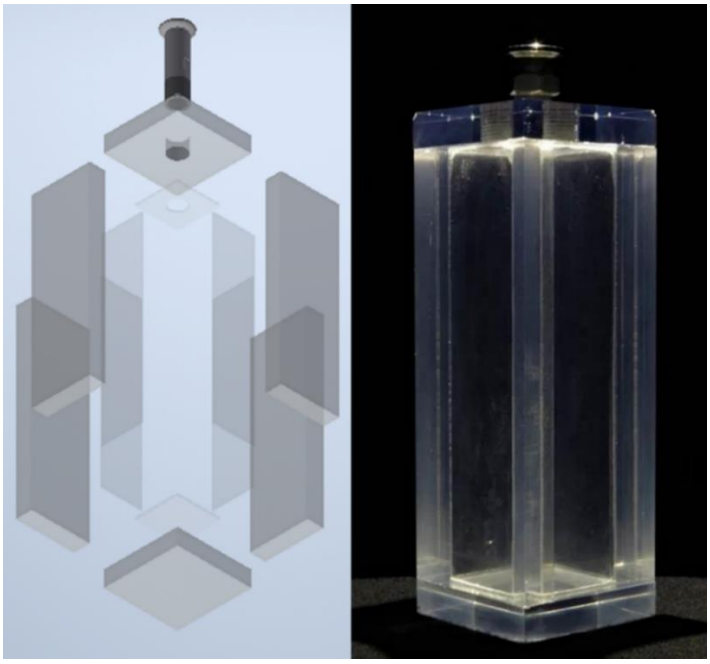

Figure 26. Turbopump detector. The dimensions of the turbopump detector were 8.4 cm by 8.4 cm by 24.6 cm. A hole was drilled through the top face with a QF16 port threaded through, used to attach the detector to the turbopump assembly. The thin scintillator lined the inside of the hollow rectangular prism, and the optically coupled thick scintillator formed the outer shell.

1 mm thick EJ-212 fast plastic scintillator with a 2.4 ns decay time and 18 mm thick EJ-240 slow plastic scintillator with a 285 ns decay time [19]. The two scintillators were constructed as a hollow rectangular prism using epoxy, with the thin dE detector lining the inside and the thick E detector forming the outer shell. The base of the detector was an 8.4 cm square, and the detector was 24.6 cm tall. A hole was drilled into one of the square sides with a QF16 port threaded through, which was used to attach the entire detector to the turbopump assembly. The side opposite the hole was optically coupled with the same optical grease used for the light guide to a 5 in. diameter ADIT B133D01 photomultiplier tube.

3.8. Total ^{66}Cu Activation

One final experiment was attempted to measure the total activation of ^{66}Cu produced by the accelerator. Immediately after activating the copper on the tungsten ribbon, the ribbon was extracted and transported to a separate detector with a known absolute efficiency. Since the half-life of ^{66}Cu was 5.12 minutes, the target had to be transported relatively quickly. Unfortunately, the turbopump for the test chamber required about 30 minutes to spin down before letting air into the chamber, which was necessary when removing the exploding wire device. Because of this, the turbopump for the test chamber was turned off before the activation process even started, and the turbopump for the 30R scattering chamber was used to keep both chambers evacuated. Then after the 30 minute activation process, the upstream faraday cup was inserted, the accelerator gate valve was closed, and the test chamber's turbopump had already spun down. The exploding wire device was removed, and the tungsten ribbon was transported so the total activation could be measured.

A group of SUNY Geneseo students used a NaI(Th) detector to detect the 1039 keV gamma rays emitted by the ^{66}Cu, and have described the procedure more fully in their report [20]. The target was transported to the detector in less than 2 minutes, so relatively little ^{66}Cu decayed before measuring the total activity. Despite the relatively quick turnover, however, the signal-to-background ratio was too low, and the experiment was unsuccessful in measuring the total ^{66}Cu activation.

Chapter 4

RESULTS

4.1. Introduction

In this chapter, the results are presented for several different experiments. Sets of experiments were carried out for the getter and turbopump systems and the growth curves or decay curves described in Chapter 2 were obtained by detecting the beta decays of ^{66}Cu or ^{20}F. Initial experiments tested whether or not the two detector systems could identify ^{66}Cu and ^{20}F. The exploding wire experiment was carried out several times, with some experiments involving the rotating shield.

4.2. Getter Trap and Detector System

The majority of experiments involved the getter system since copper was the primary target material. For the turbopump system, it was strongly suspected that copper would stick to the collection tube or turbopump blades rather than passing through to the detector, but copper would have no trouble sticking to the getter. The experiments involved detecting ^{66}Cu produced by a neutron howitzer, detecting ^{66}Cu and ^{20}F produced by the particle accelerator, and the main exploding wire experiment, with one rotating shield experiment.

4.2.1. Detecting ^{66}Cu Produced by Neutron Howitzer

Initial experiments were done using the neutron howitzer at SUNY Geneseo to test whether or not the detectors could identify ^{66}Cu before going to the effort required to produce it using the accelerator. The neutron howitzer was used to produce ^{66}Cu via ^{65}Cu(n,γ)^{66}Cu on copper strips that were then placed against the face of the getter detector. The results are shown in Figure 27, with the decay curve of ^{66}Cu on the right and the growth curve of the daughter nucleus ^{66}Zn on the left, as described in Chapter 2. The decay curve plotted the number of counts per 2 minute time bin on the vertical axis, over time in seconds on the horizontal axis. The number of counts vs. time was integrated to give the integral vs. time graph, which is the growth curve. The growth curve described in Chapter 2 was fit to the integral vs. time graph, with the fit parameters shown in Table 6. The fits for all experiments were performed using

MINUIT [21], which is part of the ROOT analysis Framework [22]. The previously measured half-life of 5.12 minutes [2] agreed with the measurement of 5.18 ± 1.18 minutes, showing that the getter detector could successfully identify ^{66}Cu by its half-life.

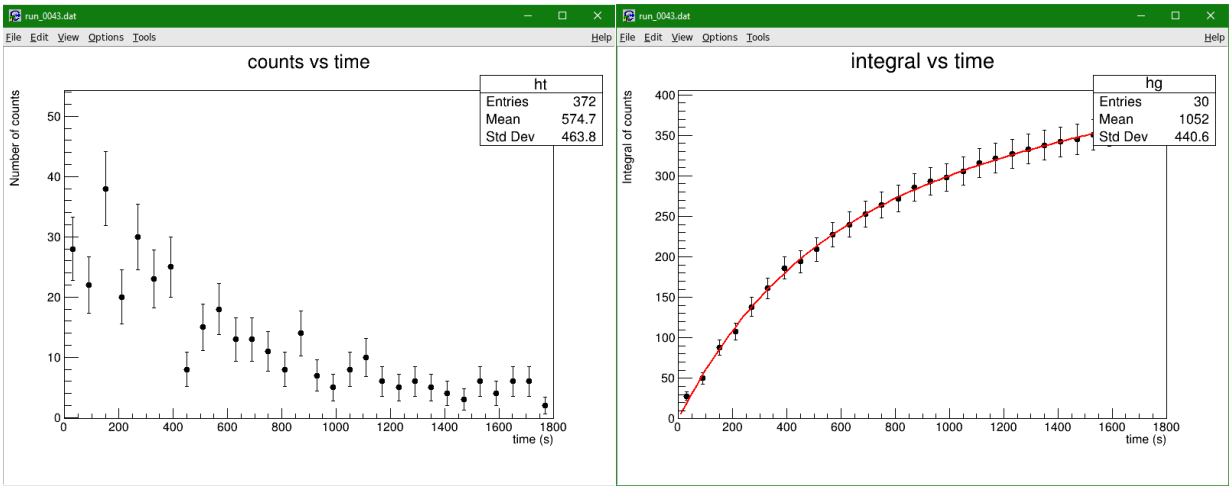

Figure 27. Results of neutron howitzer-activated ^{66}Cu using the getter detector. The decay curve described in Chapter 2 is represented by the plot on the left, showing the number of counts per 2 minute time bin on the vertical axis, over time in seconds on the horizontal axis. The growth curve from Chapter 2 has been fit to the integral of counts vs. time graph on the right, with fit parameters shown in Table 6.

Table 6. Fit parameters of the growth curve from Figure 27. The half-life was calculated using the decay constant.

$N = N_0(1 - e^{-\lambda t}) + Bt$		
	Value	Uncertainty
N_0 (decays)	269	59
λ (s^{-1})	0.00223	0.00051
B (counts/s)	0.060	0.036
$t_{\frac{1}{2}}$ (min)	5.19	1.18

4.2.2. Detecting ^{66}Cu Produced by Particle Accelerator

Before the first exploding wire experiment was carried out, attempts were made to detect ^{66}Cu directly on the tungsten ribbon with the getter detector. This was to make sure the deuteron beam was actually striking the copper and activating it via ^{65}Cu(d,p)^{66}Cu. To align

the deuteron beam, a quartz window was clipped to the copper plated tungsten ribbon and viewed with a camera through a chamber viewport. The quartz glowed when struck by the beam, so the beam could be steered and readjusted until the beam spot was over the center of the tungsten ribbon.

Once the beam was hitting the center of the tungsten ribbon, the chamber was filled with dry nitrogen and the exploding wire device was taken out so the quartz could be removed. Then the device was inserted back into the chamber, which was evacuated to a pressure of about 5×10^{-6} Torr. Then the accelerator gate valve was opened, and the deuteron beam was allowed to strike the copper for 30 minutes. Then the beam was cut off by inserting an upstream faraday cup and the getter detector was used to detect the beta decays from the ^{66}Cu on the tungsten ribbon.

Similar decay and growth curves are shown again for the accelerator-activated copper in Figure 28. A growth curve was again fit to the integral vs. time data, with results shown in Table 7. The half-life was calculated using the decay constant to be 5.23 ± 1.15 minutes, which showed that the copper on the tungsten ribbon was successfully activated and detected.

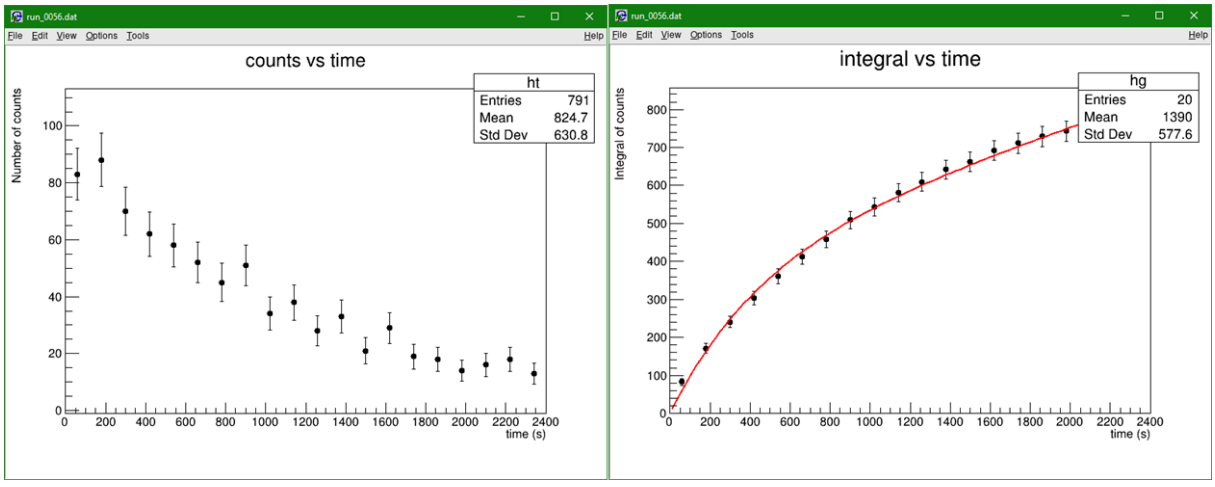

Figure 28. Results of accelerator-activated ^{66}Cu using the getter detector. The decay curve, plotting the number of counts per 2 minute time bin on the vertical axis over time in seconds on the horizontal axis, is shown on the left, and a growth curve, integrating the counts from the decay curve, is shown on the right. The growth curve described in Chapter 2, shown in red, was fit to the integral vs. time graph with results shown in Table 7.

Table 7. Fit parameters of the growth curve from Figure 28. The half-life was calculated using the decay constant.

$N = N_0(1 - e^{-\lambda t}) + Bt$		
	Value	Uncertainty
N_0 (decays)	401	73
λ (s^{-1})	0.00221	0.00048
B (counts/s)	0.178	0.037
$t_{\frac{1}{2}}$ (min)	5.23	1.15

4.2.3. Detecting ^{20}F Produced by Particle Accelerator

A similar ^{20}F detection test was carried out with Teflon tape wrapped around the tungsten ribbon and activated by the deuteron beam. Unfortunately the Teflon was never evaporated, but the getter detector was used to identify ^{20}F in situ by its half-life. Because the half-life was 11.07 s, the accelerator only irradiated the Teflon for 90 s and the beta decays were detected for 120 s.

The results from this test are shown in Figure 29, with a decay curve on the left and a growth curve on the right. However, since the half-life of ^{20}F was much shorter than that of ^{66}Cu, the beta decays were detected much faster. The electronics could not keep up with the higher count rate, leaving "gaps" in the counts vs. time graph when the Beaglebone computer needed to read out the FPGA in the FemtoDAQ. The integral vs. time graph integrated these gaps as flat lines, making it impossible to fit a growth curve. Instead, the half-life of 11.07 s was fixed for a decay curve fit, shown in red, and the other fit parameters were determined. The time bins were reduced from 2 minutes to 1 second, and the results are shown in Table 8.

4.2.4. Exploding Wire Experiment with ^{66}Cu

The exploding wire experiment was first carried out using copper as the target material with the getter system. One concern with this experiment was that not all the copper would evaporate off the tungsten. This could result in residual ^{66}Cu on the tungsten that the getter detector might detect in addition to any trapped ^{66}Cu stuck to the getter. Two thicknesses of

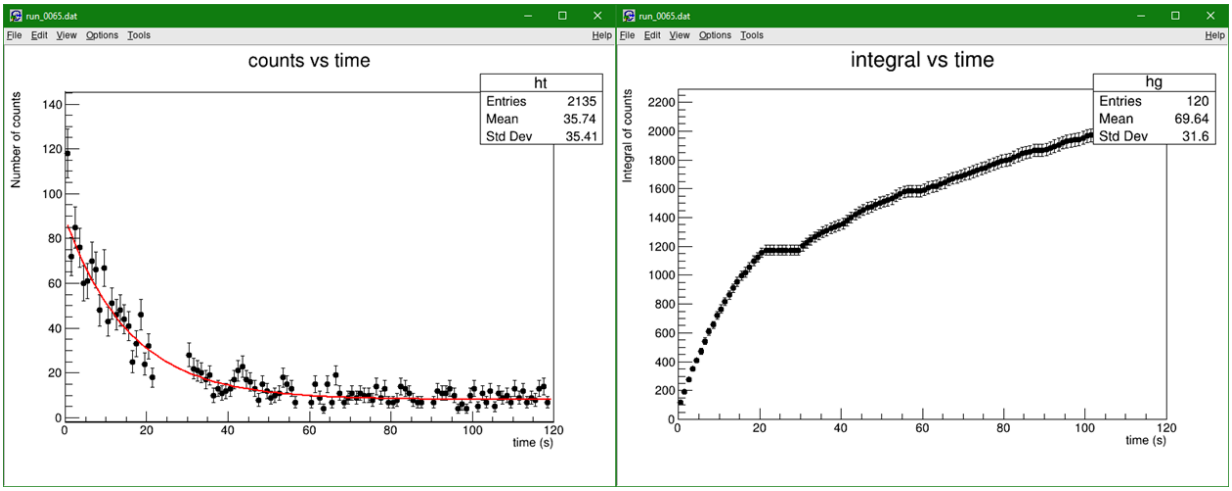

Figure 29. Results of accelerator-activated ^{20}F. The decay and growth curves described in Chapter 2 are shown in the counts vs. time and integral vs. times graphs, respectively. The high count rate led to "gaps" in the counts vs. time graph on the left, and flat lines in the integral vs. time graph on the right. Because of this, a decay curve fit was used instead of a growth curve fit, and compared to the counts vs. time graph with a fixed half-life of 11.07 s. The other fit parameters are shown in Table 8.

Table 8. Fit parameters of the decay curve from Figure 29. The total number of detected decays was calculated via $R_0 = \lambda N_0$, which was derived in Chapter 2.

$R = R_0 e^{-\lambda t} + B$		
	Value	Uncertainty
R_0 (decays/s)	80.8	2.9
λ (s^{-1})	0.0626	Fixed
B (counts/s)	8.03	0.36
N_0 (decays)	1290	46

electroplated copper were used to partially address this issue. First, a thicker 25 μm layer was used as a first attempt to maximize the amount of ^{66}Cu produced, without regard to the sticking issue. Then a thinner 11 μm layer was used as a second attempt to reduce the amount of copper that might stick to the tungsten. The thicker layer was electroplated across the entire tungsten ribbon on both sides and the thinner layer was electroplated only in a square in the center of one side of the tungsten ribbon.

The results for the 25 μm thick evaporated copper film are shown in Figure 30, with the growth curve fit parameters shown in Table 9. The half-life was calculated using the decay constant to be 5.40 ± 0.34 min, agreeing with the previously measured value of 5.12 minutes. This showed that ^{66}Cu was successfully trapped and detected by the getter system. Furthermore, visual evidence of the getter trap agreed with the results, as a layer of copper could be seen coating the getter foil after the experiment, as shown in Figure 31.

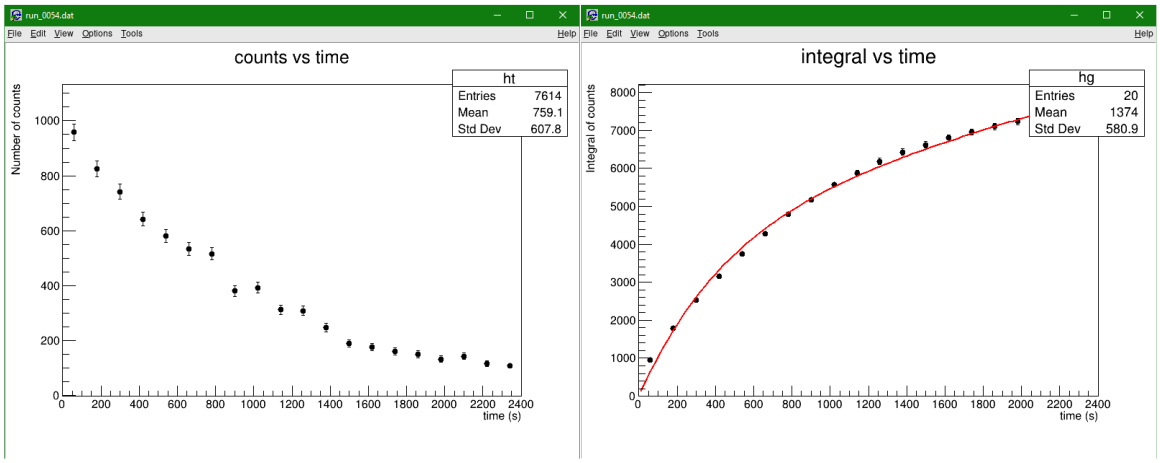

Figure 30. Results from the exploding wire experiment using 25 μm thick copper. The getter system was used to capture and detect ^{66}Cu nuclei, with the decay curve shown on the left and the growth curve shown on the right. The decay curve was represented by the number of counts per 2 minute time bin on the vertical axis, over time in seconds on the horizontal axis, and the growth curve was represented by the integral of these counts. A growth curve was fit to the integral vs. time data, with results shown in Table 9.

Table 9. Results from the growth curve in Figure 30. The half-life was calculated using the decay constant.

$N = N_0(1 - e^{-\lambda t}) + Bt$		
	Value	Uncertainty
N_0 (decays)	4635	244
λ (s^{-1})	0.00214	0.00013
B (counts/s)	1.37	0.12
$t_{\frac{1}{2}}$ (min)	5.40	0.34

Figure 31. Copper evaporated onto getter foil. This photograph, taken after several exploding wire experiments, showed that the evaporated copper had been successfully trapped by the getter foil.

The results for the 11 μm thick evaporated copper film are shown in Figure 32 with similar decay and growth curves. A growth curve fit was made to the integral vs. time data, with results shown in Table 10. The half-life was calculated using the decay constant to be 5.38 ± 0.38 minutes, which also agreed with the previously measured value, showing that the 11 μm layer of copper was successful in trapping and detecting ^{66}Cu. Furthermore, nearly the same amount of ^{66}Cu was detected as with the 25 μm layer, and the chance of any copper sticking to the target after the explosion was reduced.

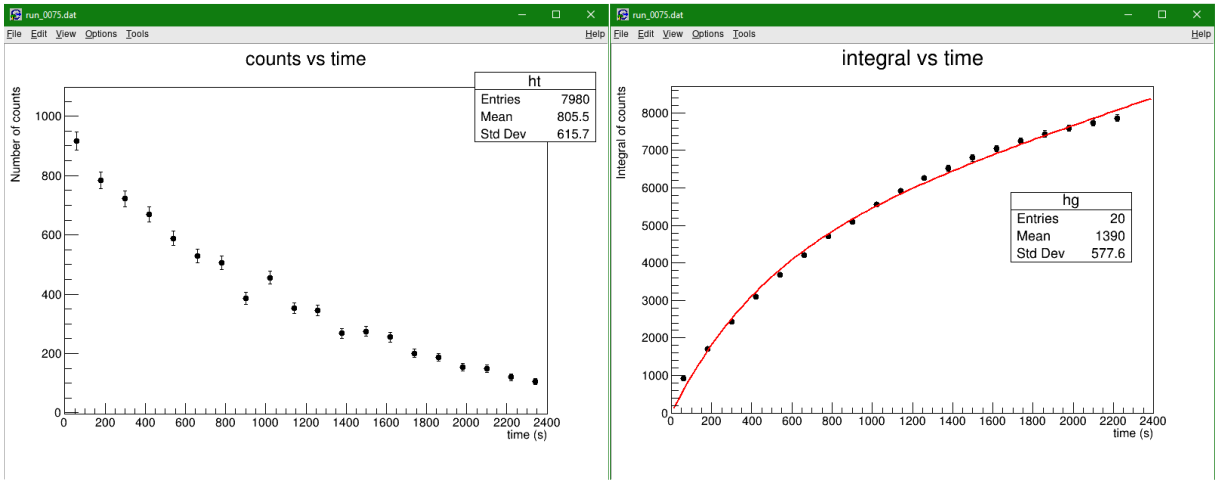

Figure 32. Results from the exploding wire experiment using 11 μm thick copper. The getter system was used to trap and detect the evaporated ^{66}Cu nuclei, with the decay curve shown on the left and the growth curve shown on the right. The same 2 minute time bins were used, and a growth curve was fit to the integral vs. counts data, with results shown in Table 10.

Table 10. Results from the growth curve in Figure 32. The half-life was calculated using the decay constant.

$N = N_0(1 - e^{-\lambda t}) + Bt$		
	Value	Uncertainty
N_0 (decays)	4171	249
λ (s^{-1})	0.00215	0.00015
B (counts/s)	1.78	0.13
$t_{\frac{1}{2}}$ (min)	5.38	0.38

4.2.5. Rotating Shield

The question of whether or not copper was sticking to the tungsten after the explosion was addressed more fully with an experiment involving the rotating shield. The shield was used to "catch" the evaporating copper and then move it far away from the getter detector, repeating the exploding wire experiment but without trapping any ^{66}Cu nuclei on the getter foil. An 11 μm thick layer of copper was activated by the deuteron beam and evaporated onto the shield, shown in Figure 33, which rested between the target and the getter. The shield was then rotated to its default position in front of the test chamber's turbopump, "far away" from the getter detector. The getter detector was then used to count the decays from any ^{66}Cu left on the tungsten, although it could possibly detect some ^{66}Cu splattered elsewhere in the chamber or on the "far away" shield.

The results from the rotating shield experiment are shown below in Figure 34. As expected, the counts vs. time and integral vs. time graphs showed hardly any decays, since ^{66}Cu was not trapped by the getter foil. To determine the amount of ^{66}Cu that was detected, however, decay and growth curves were fit to the appropriate histograms, with fixed decay constants corresponding to 5.12 minute half-lives. The results from the fits are shown in Table 11. When compared with the exploding wire experiment using an 11 μm thick copper film, the rotating shield experiment revealed that very little, if any, ^{66}Cu was detected on the tungsten ribbon after the explosion. Moreover, after each exploding wire experiment, there appeared to be no copper stuck on the tungsten ribbons, as shown in Figure 35 with tungsten ribbons from two different exploding wire experiments.

Figure 33. Copper evaporated onto the rotating shield. The rotating shield was used to "catch" the evaporated copper and then move it far away from the getter detector. This allowed the getter detector to isolate the tungsten ribbon as the main source of any ^{66}Cu, to determine whether or not any copper stuck to the tungsten after it was evaporated.

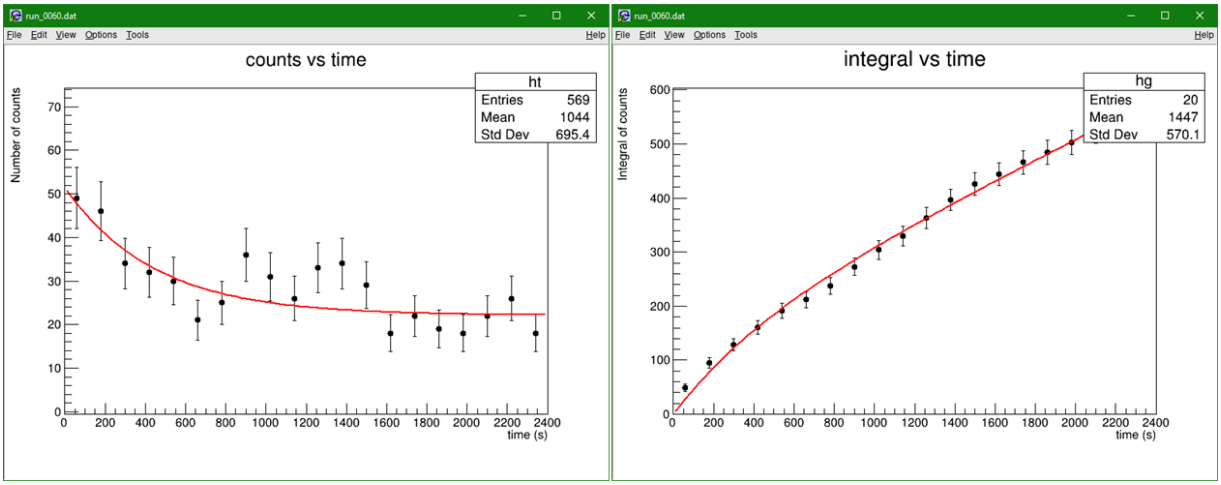

Figure 34. Results from the rotating shield experiment. The ^{66}Cu was evaporated on to the rotating shield, which then rotated 120 degrees back toward the opposite side of the test chamber. The getter detector was used to detect any residual ^{66}Cu on the target but may have also been exposed to ^{66}Cu elsewhere in the chamber. Decay (left) and growth (right) curve fits were made with fixed decay constants corresponding to 5.12 minute half-lives to determine the total amount of ^{66}Cu detected. Results are shown in Table 11.

Table 11. Results from the decay and growth curve fits from Figure 34. For the decay and growth curves, respectively, N_0 and R_0were calculated using the $R_0 = \lambda N_0$ relationship. The decay constant was fixed to correspond to a 5.12 minute half-life.

	$R = R_0 e^{-\lambda t} + B$		$N = N_0(1 - e^{-\lambda t}) + Bt$	
	Value	Uncertainty	Value	Uncertainty
R_0 (decays/s)	0.245	0.048	0.303	0.031
N_0 (decays)	109	21	134	14
B (counts/s)	0.184	0.012	0.188	0.010
λ (s^{-1})	0.00226	Fixed	0.00226	Fixed

Figure 35. Tungsten ribbons after exploding wire experiments. No macroscopic amounts of copper could be seen on the post-explosion tungsten ribbons, as supported by results from the rotating shield experiment.

4.3. Turbopump Trap and Detector System

Before the exploding wire experiment was conducted using the turbopump system, the turbopump detector was used to detect ^{66}Cu produced by the neutron howitzer. This experiment was similar to the one done using the getter detector, and similar decay and growth curves are shown in Figure 36. Data were collected over 1 minute time bins, and a growth curve was fit to the integral vs. time data, with results shown in Table 12. The half-life was calculated using the decay constant to be 5.08 $\pm$ 0.35 minutes. This half-life agreed with the previously measured value of 5.12 minutes, demonstrating that the turbopump detector could successfully identify ^{66}Cu.

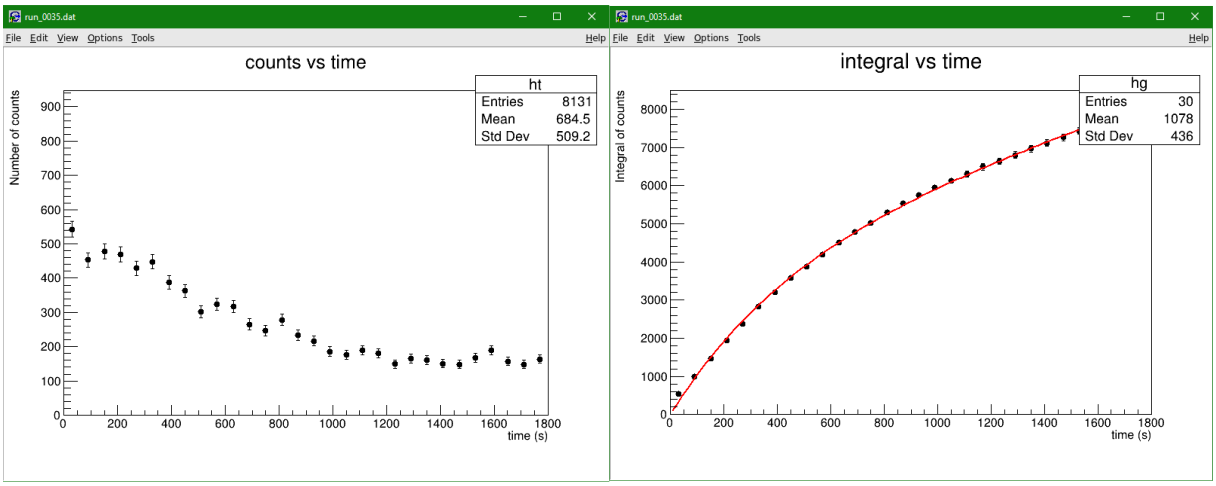

Figure 36. Results of neutron howitzer-activated ^{66}Cu using the turbopump detector. A decay curve is shown on the left, plotting the number of counts per 1 minute time bin on the vertical axis, over time in seconds on the horizontal axis. A growth curve, plotting the integral of the number of counts over time, is shown on the right. A growth curve was fit to the integral vs. time data, with results shown in Table 12.

Table 12. Results from the growth curve in Figure 36. The half-life was calculated using the decay constant.

$N = N_0(1 - e^{-\lambda t}) + Bt$		
	Value	Uncertainty
N_0 (decays)	3956	265
λ (s^{-1})	0.00227	0.00016
B (counts/s)	2.37	0.16
$t_{\frac{1}{2}}$ (min)	5.08	0.35

After the initial ^{66}Cu detection test, the exploding wire experiment was carried out once more using the turbopump system. Copper was electroplated onto the center of one side of the tungsten ribbon with a thickness of 11 μm. Unlike the previous experiments, the turbopump in the turbopump system was used to help evacuate the test chamber. Once the chamber was evacuated, the copper was irradiated for 30 minutes, the upstream Faraday cup was inserted, the accelerator gate valve was closed, and the modified procedure for the turbopump system began. First Valve 2 was closed, cutting off the turbopump from the fore pump. Then Valve 1 was opened, creating a pathway between the turbopump outlet and the

detector. Then the tungsten was heated for 10 seconds, evaporating the copper. Valve 1 remained open for an additional 10 seconds, then closed, and data were collected for 40 minutes.

The results from the turbopump system are shown in Figure 37. As data were being collected, the number of counts per 2 minute time bin were monitored using the turbopump detector. Within the first few minutes, it was apparent that the turbopump detector was only detecting a constant background of approximately 200 counts per time bin. The accelerator team was allowed to briefly take out the Faraday cup at around 800 seconds to run additional tests of their own, which led to higher background counts in the time bin around the 800 s mark. Regardless, an attempt was made to fit a growth curve to the integral vs. time data, with a fixed decay constant corresponding to a half-life of 5.12 minutes. The results of the growth curve fit are shown in Table 13. When compared to the neutron howitzer activation test, not that the two can be compared directly, of course, it seemed like the turbopump system was unsuccessful in trapping ^{66}Cu. As expected, the expanding copper likely stuck to the collection tube or turbopump blades. A photograph of the end of the collection tube, in Figure 38, showed that copper stuck to the rim of the collection tube, demonstrating that the experiment was successful in evaporating copper toward the turbopump system.

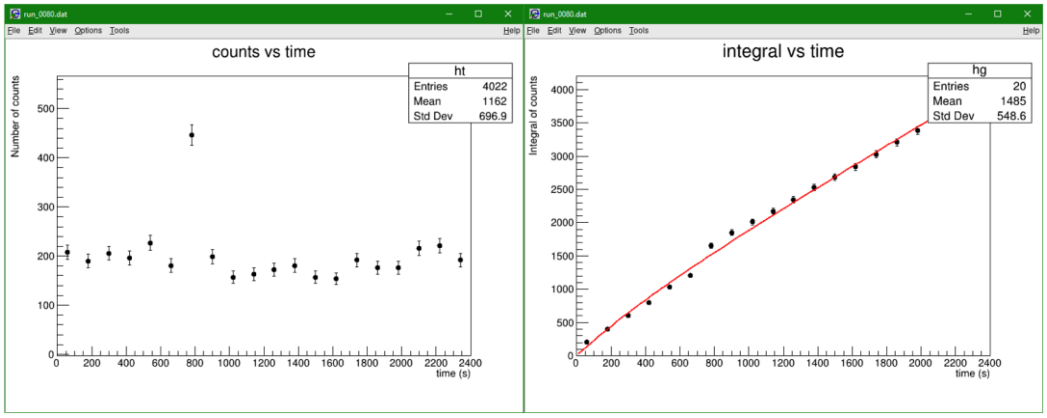

Figure 37. Results of exploding wire experiment using the turbopump system. The decay curve on the left appears to only show a constant background of about 200 counts per 2 minute time bin, indicating that little to no ^{66}Cu was detected. The integral vs. time graph appears to show the same, but a growth curve with a fixed decay constant corresponding to a 5.12 minute half-life was fit to measure any trapped ^{66}Cu nuclei. Results of the fit are shown in Table 13.

Table 13. Results of the growth curve fit in Figure 37. The decay constant was fixed to correspond to a 5.12 minute half-life.

$N = N_0(1 - e^{-\lambda t}) + Bt$		
	Value	Uncertainty
N_0 (decays)	367	33
λ (s^{-1})	0.00226	Fixed
B (counts/s)	1.55	0.024
$t_{\frac{1}{2}}$ (min)	5.12	Fixed

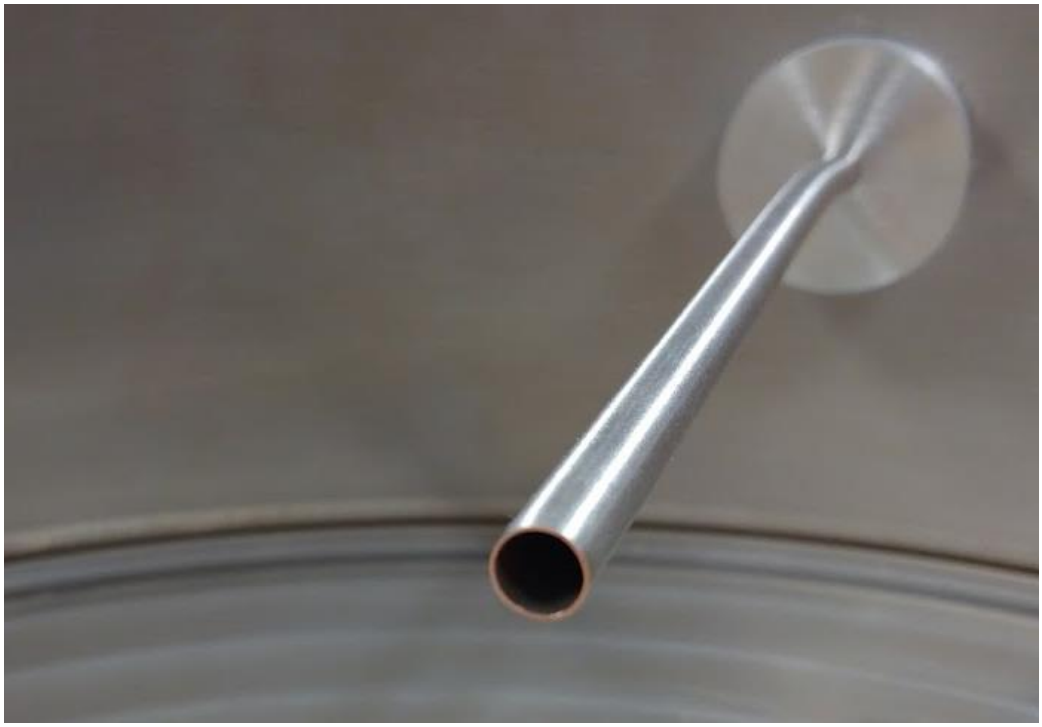

Figure 38. Copper evaporated onto turbopump system's collection tube. A coating of copper was visible on the rim of the collection tube, indicating that the experiment had been successful in evaporating copper toward the turbopump system, even if no ^{66}Cu was detected.

Chapter 5

CONCLUSION

5.1. Summary

The long term goal of this research is to measure the low energy nuclear cross sections of light ion reactions using ICF. These measurements can be made by trapping and detecting the radioactive isotopes produced in ICF implosions as they expand outward in a neutral gas. Two trap and detector systems, a getter system and a turbopump system, have been proposed for ICF experiments to measure these cross sections and were tested in a small scale "exploding wire" experiment. The exploding wire experiment involved evaporating radioactive copper inside a test chamber, producing a radioactive expanding gas similar in some respects to the gas resulting from ICF implosions, trapping the gas, and detecting the beta decays of the radioactive nuclei.

5.1.1. Summary of Experiments

Several experiments were conducted using both the getter and turbopump systems. The first of these involved detecting ^{66}Cu produced by SUNY Geneseo's neutron howitzer to determine whether or not the detectors could identify ^{66}Cu by its half-life. The second set of experiments involved detecting in situ ^{66}Cu or ^{20}F produced by the accelerator to determine whether or not the material coating the "exploding wire" could be activated. Lastly, the exploding wire experiment was conducted using copper as the target material with each detector. One experiment in which the target material was evaporated involved a rotating shield, which helped demonstrate that nearly all the radioactive copper had evaporated off the target. The results of each experiment are summarized in Table 14.

The first two ^{66}Cu detection tests using the neutron howitzer determined that both the getter and turbopump detectors could identify ^{66}Cu by its half-life. The turbopump detector detected nearly 15 times more ^{66}Cu than the getter detector because it is a nearly 4π solid angle detector. The next two tests using the getter detector and the accelerator revealed that ^{66}Cu and ^{20}F could both be successfully activated on the tungsten ribbon. The total amount

of ^{20}F activation appeared to be higher than the total amount of ^{66}Cu activation. The next two tests, where copper was "exploded" as the target material revealed that the getter system could successfully trap and detect the evaporated ^{66}Cu. In each test, the getter detector detected over 10 times more ^{66}Cu nuclei than when it was just used to detect ^{66}Cu on the target a few centimeters away. The next experiment involving the rotating shield showed that very little, if any, ^{66}Cu remained on the tungsten ribbon after heating it, indicating that the ^{66}Cu detected in the exploding wire experiment was indeed from trapped copper. The last experiment showed that the turbopump system was unsuccessful in trapping the evaporated ^{66}Cu, as the copper most likely stuck to its components before reaching the detector.

Table 14. Summarized results from all experiments. For each experiment, the target material, activation method, detector used, type of curve fit, and all fit parameters are shown. The fit parameters include the total number of detected decays N_0, the initial decay rate R_0, the background rate B, the decay constant λ, and the half-life $t_{1/2}$.

Material	Activation	Detector	Fit Type	N_0 (Decays)	R_0 (Decays/s)	B (Counts/s)	λ (s^{-1})	$t_{1/2}$ (min)
Copper	Howitzer	Getter	Growth	269 ± 59	0.60 ± 0.19	0.06 ± 0.04	0.00223 ± 0.00051	5.19 ± 1.181
Copper	Howitzer	Turbopump	Growth	3956 ± 265	9.00 ± 0.86	2.37 ± 0.16	0.00227 ± 0.00016	5.08 ± 0.347
25 µm Cu	Accelerator	Getter	Growth	401 ± 73	0.88 ± 0.25	0.18 ± 0.04	0.00221 ± 0.00048	5.23 ± 1.146
Fluorine	Accelerator	Getter	Decay	1290 ± 46	80.77 ± 2.90	8.03 ± 0.36	0.06262 (Fixed)	0.18 (Fixed)
(Evaporated) 25 µm Cu	Accelerator	Getter	Growth	4635 ± 244	9.92 ± 0.81	1.37 ± 0.12	0.00214 ± 0.00013	5.4 ± 0.337
(Evaporated) 11 µm Cu	Accelerator	Getter	Growth	4171 ± 249	8.95 ± 0.83	1.78 ± 0.13	0.00215 ± 0.00015	5.38 ± 0.379
(Evaporated - Shield) 11 µm Cu	Accelerator	Getter	Growth	134 ± 14	0.30 ± 0.03	0.19 ± 0.01	0.00226 (Fixed)	5.12 (Fixed)
(Evaporated - Shield) 11 µm Cu	Accelerator	Getter	Decay	109 ± 21	0.25 ± 0.05	0.18 ± 0.01	0.00226 (Fixed)	5.12 (Fixed)
11 µm Cu	Accelerator	Turbopump	Growth	367 ± 33	0.83 ± 0.07	1.55 ± 0.02	0.00226 (Fixed)	5.12 (Fixed)

One additional experiment, described in Chapter 3, was designed to measure the total ^{66}Cu activation in the copper film by counting the number of 1039 keV gamma rays using an NaI(Th) detector with known absolute efficiency. Unfortunately, the background radiation was too high to accurately measure the total ^{66}Cu activation, so the experiment was unsuccessful. This measurement would have been used along with the number of trapped and detected ^{66}Cu nuclei from the exploding wire experiment to determine the total fraction of expanding radioactive nuclei that were trapped and detected by the getter system. Of course, the expanding gas in the exploding wire experiment was not isotropic like the gas in

an ICF implosion, but this fraction could help in understanding the efficiency of the getter system when implemented in an ICF experiment.

5.2. Future Plans

The future plans for this experiment involve testing lithium and fluorine as possible target materials, using new electronic systems to process and digitize data at a faster rate, and experiments to determine the total activation of radioactive nuclei produced in each target material. Lithium would be especially important as a target material since the reaction product, ^{8}Li, is one of the relevant reaction products for ICF experiments (see Table 1 and 2). Future OMEGA ride-along experiments could also be performed to test the electronics and detector systems more thoroughly.

A vacuum deposition system is currently being developed to deposit ^{7}Li onto the tungsten ribbon in the test chamber for future exploding wire experiments. Once the tungsten ribbon is coated with a layer of ^{7}Li, the deuteron beam could activate the lithium via ^{7}Li(d,p)^{8}Li, and the current pulse heating the tungsten could evaporate ^{8}Li atoms out toward the trap and detector systems. The beta decays of the trapped ^{8}Li would be detected, just as they were for the trapped ^{66}Cu.

The same exploding wire experiment could be repeated with the tungsten ribbon wrapped in Teflon tape, so ^{20}F could be trapped and detected. This experiment would be a useful test for the turbopump system, since when pyrolyzed, fluorine gas becomes relatively inert and would be more likely to reach the turbopump detector. An experiment to activate ^{20}F and detect its decays in situ was already carried out, but there was difficulty with the electronics due to the small FemtoDAQ memory and slow readout speed. These issues led to “gaps” in the data during the readout periods, making it difficult to fit decay or growth curves.

An upgraded electronic system with more memory and a faster readout speed could be tested in both ^{8}Li and ^{20}F experiments. A new CAEN 730 Waveform Digitizer and SkuTek FemtoDAQ+ could potentially meet the demands of future experiments. The digitizer would read data using a Flash ADC with a 14-bit resolution and 500 MS/s sampling rate, and the FemtoDAQ+ would upgrade the low end Spartan-6 LX9 FPGA of the current system to a more

powerful Artix-7 200T, in which the FPGA would gain an additional 16 MB memory buffer. The on-chip event buffer and waveform memory would be upgraded from 64 kB to 1.4 MB, and the off-chip RAM would be upgraded from 512 kB to 2 MB. Other parameters of the off-chip RAM, such as the memory port, would be upgraded from 8 bits to 32 bits, and the clock speed from 100 MHz to 200 MHz. The new electronic system would potentially eliminate the readout issues from the ^{20}F experiment and from previous OMEGA ride-along experiments.

Another OMEGA ride-along experiment would be useful in testing the new electronics, as well as testing the detector systems more thoroughly. In particular, the turbopump detector should be tested with more shielding and with its contents evacuated. From the previous OMEGA ride-along experiment, neutron reactions produced in the air inside the turbopump were most likely a significant source of background radiation. In an actual ICF experiment, however, the turbopump detector would be evacuated, so these previously detected neutron reactions would not be present. Furthermore, the background radiation following an ICF implosion could be more carefully measured using each detector with the upgraded electronic systems.

Lastly, the experiment to measure total ^{66}Cu activation should be performed again, perhaps with extra shielding to eliminate background radiation, making the signal-to-background ratio higher for the 1039 keV gamma rays. This measurement would be required to determine the fraction of ^{66}Cu nuclei trapped and detected by the getter system in the exploding wire experiment. Additionally, experiments to measure the total activation of ^{8}Li and ^{20}F would be beneficial but would require an in situ detector with a known absolute efficiency, which has not yet been designed.

Overall, the experiments conducted were successful in trapping and detecting radioactive isotopes produced in a small-scale exploding wire experiment. The fraction of trapped and detected reaction products was not yet measured, however, so future experiments would be required to determine the absolute efficiency of each trap and detector system. Once this fraction is measured, the getter and turbopump systems could perhaps be used in the proposed ICF experiments to measure the low energy nuclear cross sections of various light ion reactions.

Appendix A

C CODE USED TO ANALYZE PHOSWICH DETECTOR DATA

```
   #include <iostream>

   //
========================================
========================================
=====
   // Subroutine to read data from run
file, fill histograms and ntuple
   //
========================================
========================================
=====

   void read_file(TString fname, Int_t
*cuts, TH1F *h0, TH1F *h1, TH2F *h01,
TH1F *ht, TNtuple *ntuple, float offset)
{

   char cline[256];
      // input line buffer

   // data from Femtodaq

   Int_t adc0,adc1;
   long timestamp;
   float dE1,dE2,dE3,dE4;
   float E1,E2,E3,E4;
   float m1,m2,m3,m4,b1,b2,b3,b4;


   printf("Opening input file: %s   ",
fname.Data());
   ifstream in;
   in.open(fname.Data());

   // Read in the first 10 comment lines
2.3906*10^
   for (int i=1; i<10; i++) {
      in.getline(cline,256);
      //printf("%s",cline);
      //cout<<"line"<<i<<":
"<<cline<<endl;

      }


   // number of data lines read in from
each file
   Int_t nlines = 0;

   // Read in data and fill histograms
and ntuple
   do {
      in >> timestamp>>adc0>>adc1;
      //printf("in fail =
%d\n",in.fail());

      if (in.fail()) break;
      //timestamp = (decay_func-
>GetRandom()+0.2)*1000.;  // test
function

      if (nlines < 5) printf("%d
time=%ld  adc0=%d adc1=%d
\n",in.good(),timestamp,adc0,adc1);
      //printf("%d %d  time=%ld  adc0=%d
adc1=%d \n",nlines,
in.good(),timestamp,adc0,adc1);

      if ( (adc0 < 2051) || (adc1 <
2051) ){
      h0->Fill(adc0);      //  hist dE
      h1->Fill(adc1);      //  hist E
      h01->Fill(adc1,adc0);       // dE
vs E
      }

      dE1 = cuts[0];
      dE2 = cuts[1];
      dE3 = cuts[3];
      dE4 = cuts[4];
      E1 = cuts[5];
      E2 = cuts[6];
      E3 = cuts[7];
      E4 = cuts[8];

   //  printf("1 %f %f 2 %f %f 3 %f %f 4
%f %f\n",E1,dE1,E2,dE2,E3,dE3,E4,dE4);
   //
   //(E2,dE2)               (E3,dE3)
   //
   //
   //
   // (E1,dE1)               (E4,dE4)
   //

      m1 = (float)(dE2-dE1)/(E2-E1);
      b1 = dE1 - m1*E1;
      m2 = (float)((dE3-dE2)/(E3-E2));
      b2 = dE2 - m2*E2;
```

```
      m3 = (float)(dE4-dE3)/(E4-E3);
      b3 = dE3 - m3*E3;
      m4 = (float)(dE1-dE4)/(E1-E4);
      b4 = dE4 - m4*E4;

      //printf("x %d y %d m %6.2f  b
%6.2f  m2 *x + b cut %6.1f\n",adc1,adc0,
m2, b2, m2*adc1+b2);

      if ( (adc1 > (adc0-b1)/m1 ) &&
(adc1 < (adc0-b3)/m3 ) &&
(adc0<m2*adc1+b2) && (adc0>m4*adc1+b4) )
{
      //if ( (adc0 < 2051) || (adc1 <
2051) ){

      ht->Fill(
(float)((timestamp)/1.0e8)-offset  );

      }

      ntuple->Fill(timestamp,adc0,adc1);

      nlines++;

     } while(!in.eof());

   printf(" found %d points\n",nlines);
   //printf("start=%ld  \n",start);
   //printf("time=%ld  adc0=%d adc1=%d
\n",timestamp,adc0,adc1);

   in.close();
   }


   //
=========================================
=========================================
=====
   // Main
   //
=========================================
=========================================
=====

   void analyze(TString fname="test") {
   //  read in and analyzed data from
decay_exp.py
   //  created: 07/2016 Mark Yuly
   //  modified: 01/19/2017 Mark Yuly
read in data saved by new FemtoDAQ FPGA
program

   // ========== USER SETTABLE VALUES
==============================
   // length of run in seconds
   Int_t run_length = 1800;

   // size of time bin (ms)
   Int_t time_bin_size =60000;

   // cut on dE-E to make the time
histogram
   //
   //(E2,dE2)               (E3,dE3)
   //
   //
   //
   // (E1,dE1)               (E4,dE4)
   //

   //Int_t dE1 =0; Int_t E1 = 0;
   //Int_t dE2 =2000; Int_t E2 = 0;
   //Int_t dE3 = 2001; Int_t E3 = 2500;
   //Int_t dE4 =0; Int_t E4 =2501;

   // Int_t dE1 =500; Int_t E1 = 200;
   // Int_t dE2 =1800; Int_t E2 = 400;
   // Int_t dE3 = 2200; Int_t E3 = 2050;
   // Int_t dE4 = 1300; Int_t E4 =2001;

   Int_t dE1 =250; Int_t E1 = 150;
   Int_t dE2 = 2202; Int_t E2 =701;
   Int_t dE3 = 2300; Int_t E3 = 2001;
   Int_t dE4 =251; Int_t E4 = 2000;

   //Int_t dE1 =1000; Int_t E1 = 300;
   //Int_t dE2 = 2202; Int_t E2 =301;
   //Int_t dE3 = 2300; Int_t E3 = 2001;
   //Int_t dE4 =1100; Int_t E4 = 2000;

   Int_t cuts[9];


      cuts[0] = dE1;
      cuts[1] = dE2;
      cuts[3] = dE3;
      cuts[4] = dE4;
      cuts[5] = E1;
      cuts[6] = E2;
      cuts[7] = E3;
      cuts[8] = E4;



   // scale factor for calibration
   float scalex =260;
   float scaley = 600;
   int off_x= 350;
   int off_y=1200;

   //
=========================================
=========================
```

```
    TString run_file;       // list of
run file names to process
    int numlist;                    //
number of files to process
    float offset;                   //
offset for each run
    int in_run_num;         // run number
to input
    char buffer[100];       // temporary
buffer
    char last_buffer[100];          //
temporary buffer of last item processed

    char cline[256];
        // input line buffer
    char str[30];
              // char string buffer

    // calibration data for energy
deposited in each detector
    float T[17]={
0.35,0.4,0.45,0.5,0.55,0.6,0.7,0.8,0.9,1,
1.25,1.5,1.75,2,2.5,3,3.5};
    float
dE_CSDA[17]={0.306,0.256,0.236,0.224,0.21
5,0.209,0.201,0.196,0.192,0.190,0.187,0.1
86,0.186,0.186,0.187,0.189,0.192};
    float
E_CSDA[17]={0.044,0.144,0.214,0.276,0.335
,0.391,0.499,0.604,0.708,0.810,1.063,1.31
4,1.564,1.814,2.313,2.811,3.308};
    float
dE_proj[17]={0.350,0.259,0.239,0.228,0.22
1,0.216,0.211,0.207,0.205,0.204,0.202,0.2
00,0.200,0.199,0.199,0.199,0.199};
    float E_proj[17]
={0.000,0.141,0.211,0.272,0.329,0.384,0.4
89,0.593,0.695,0.796,1.048,1.300,1.550,1.
801,2.301,2.801,3.301};
    int print_e[17]={
0,1,0,0,0,1,0,0,1,0,1,1,1,1,1,1,1};

    printf("Opening run run file: %s\n",
fname.Data());

    // number of time bins
    Int_t num_time_bin =
run_length*1000./time_bin_size ;
    printf("Number of time bins
%d\n",num_time_bin);

    // exponential decay + background fit
function
    TF1 *decay_func = new
TF1("decay","[0]*exp(-
[1]*x)+[2]*x+[3]",0.,run_length);

    // exponential growth + background
fit function
    TF1 *grow_func = new
TF1("growth","[0]*(1-exp(-
[1]*x))+[2]*x+[3] + [4]*(1-exp(-
[5]*x))",0.,run_length);

    // create the histograms
    TString root_name = fname;
    root_name.Append(".root");
    TFile *f = new
TFile(root_name,"RECREATE");
    TH1F *h0 = new
TH1F("h0","ADC0_spectrum",4000,0,3999);
    h0->SetFillColor(0);
    TH1F *h1 = new
TH1F("h1","ADC1_spectrum",4000,0,3999);
    h1->SetFillColor(0);
    TH2F *h01 = new TH2F("h01","ADC0 vs
ADC1",4000,0,3999,4000,0,3999);
    h01->SetFillColor(0);
    TH1F *ht = new TH1F("ht","counts vs
time",num_time_bin,0.,run_length);
    ht->SetFillColor(0);
    TH1F *hg = new TH1F("hg","integral vs
time",num_time_bin,0.,run_length);
    hg->SetFillColor(0);

    // create the root tree for output
root file
    TNtuple *ntuple = new
TNtuple("ntuple","data from ascii
file","timestamp,adc0,adc1");

    //Either open a single run file, or
loop through a list of run files
    if (fname(0,3)=="run") {       //
single run file
       printf("Opening run run file:
%s\n", fname.Data());
       offset = 0;
       read_file(fname, cuts, h0, h1,
h01, ht, ntuple, offset);
       printf(" File opened and read
successfully.\n");
       }
    else {
       printf("Opening run list file:
%s\n", fname.Data());
       ifstream in_list;
       in_list.open(fname.Data());

       // number of data lines read in
from each file
            numlist = 0;
```

```
	// Read in the file names and
offsets
	do {
	in_list >> offset>>in_run_num;

	sprintf(buffer,"run_%04d.dat",in_r
un_num);
	//cout<<offset<<in_run_num<<endl;
	run_file=buffer;
	//printf("[%s]",run_file.Data());

		//if (numlist < 50)
printf("%d  %s  %4.2f
\n",in_list.good(),run_file.Data(),offset
);
		if (buffer[7] !=
last_buffer[7]) read_file(run_file, cuts,
h0, h1, h01, ht, ntuple, offset);
		numlist++;
		strcpy(last_buffer,
buffer);
	} while (!in_list.eof());

	printf(" Found %d runs in
list\n",numlist);
	}



    // Show histograms of dE E and 2D
    TCanvas *c1 = new
TCanvas("c1",fname.Data(),200,10,800,600)
;
    c1->SetFillColor(0);

    TPad *pad1 = new
TPad("pad1","ADC0",0.03,0.62,0.50,0.92,21
);
    pad1->SetFillColor(0);
    TPad *pad2 = new
TPad("pad2","ADC1",0.51,0.62,0.98,0.92,21
);
    pad2->SetFillColor(0);
    TPad *pad3 = new TPad("pad3","ADC0 vs
ADC1",0.03,0.02,0.97,0.57,21);
    pad3->SetFillColor(0);
    pad1->Draw();
    pad2->Draw();
    pad3->Draw();

    pad1->SetBottomMargin(0.15);
    pad1->SetLeftMargin(0.14);
    pad2->SetBottomMargin(0.15);
    pad2->SetLeftMargin(0.14);

    h0->GetXaxis()->SetTitle("dE
(ADC0)");
    h0->GetXaxis()->SetLabelSize(0.06);
    h0->GetXaxis()->SetTitleSize(0.06);
    h0->GetYaxis()->SetTitle("Number of
counts");
    h0->GetYaxis()->SetLabelSize(0.06);
    h0->GetYaxis()->SetTitleSize(0.06);
    h0->GetYaxis()->SetTitleOffset(1.1);

    h1->GetXaxis()->SetTitle("E (ADC1)");
    h1->GetXaxis()->SetLabelSize(0.06);
    h1->GetXaxis()->SetTitleSize(0.06);
    h1->GetYaxis()->SetTitle("Number of
counts");
    h1->GetYaxis()->SetLabelSize(0.06);
    h1->GetYaxis()->SetTitleSize(0.06);
    h1->GetYaxis()->SetTitleOffset(0.8);

    h01 -> SetYTitle("dE (ADC0)");
    h01->GetYaxis()->SetTitleOffset(0.9);
    h01 -> SetXTitle("E (ADC1)");
    //h01->GetYaxis()->SetRange(1000,
2200);
    //h01->GetXaxis()->SetRangeUser(300,
2000.);

    pad1->cd();
    h0->Draw();
    pad2->cd();
    h1->Draw();
    pad3->cd();
    h01->Draw();
    pad3->Draw();
    c1->Update();

    // Mark the cut region
    TLine *line1 = new
TLine(E1,dE1,E2,dE2);
    line1->SetLineColor(kGreen);
    line1->Draw();

    TLine *line2 = new
TLine(E2,dE2,E3,dE3);
    line2->SetLineColor(kGreen);
    line2->Draw();

    TLine *line3 = new
TLine(E3,dE3,E4,dE4);
    line3->SetLineColor(kGreen);
    line3->Draw();

    TLine *line4 = new
TLine(E4,dE4,E1,dE1);
    line4->SetLineColor(kGreen);
    line4->Draw();


    //Show decay histogram vs time and
fit histogram
```

```
   TCanvas *c2 = new
TCanvas("c2",fname.Data(),200,10,800,600)
;

   gPad->SetBottomMargin(0.15);
   ht->GetYaxis()->SetTitle("Number of
counts");
   ht->GetXaxis()->SetTitle("time (s)");
   gStyle->SetErrorX(0.0001);
   ht->SetLineColor(kBlack);
   ht->SetMarkerStyle(20);
   ht->SetFillColor(kGreen);
   ht->GetXaxis()->SetLabelSize(0.03);
   ht->GetXaxis()->SetTitleSize(0.03);
   ht->GetYaxis()->SetLabelSize(0.03);
   ht->GetYaxis()->SetTitleSize(0.03);
   ht->GetYaxis()->SetTitleOffset(1.7);

   ht->GetYaxis()->SetRangeUser(0,
70000);

   ht->Draw("E1");
   gPad->Draw();
   c2->Update();

   //Show growth histogram vs time and
fit histogram
   TCanvas *c3 = new
TCanvas("c3",fname.Data(),200,10,800,600)
;

   gPad->SetBottomMargin(0.15);
   hg->GetYaxis()->SetTitle("Integral of
counts");
   hg->GetXaxis()->SetTitle("time (s)");
   gStyle->SetErrorX(0.0001);
   hg->SetLineColor(kBlack);
   hg->SetMarkerStyle(20);
   hg->SetFillColor(kGreen);
   hg->GetXaxis()->SetLabelSize(0.03);
   hg->GetXaxis()->SetTitleSize(0.03);
   hg->GetYaxis()->SetLabelSize(0.03);
   hg->GetYaxis()->SetTitleSize(0.03);
   hg->GetYaxis()->SetTitleOffset(1.7);

   //hg->GetYaxis()->SetRangeUser(0,
70000);
   hg->SetMinimum(0);

   int integ=0;
   for (int i=0;i<num_time_bin;i++) {
      integ=integ + ht-
>GetBinContent(i);
      hg->SetBinContent(i,integ);
      }

   hg->Draw("E1");
   gPad->Draw();

   c3->Update();

   // write the histogram and ntuples to
root file
   f->Write();


   }
```

Appendix B

FEMTODAQ PYTHON CODE RUNNING ON BEAGLEBONE

```
#!/usr/bin/python

# SLICS.py
# Short-Lived Isotope Counting System
# (c) 2019 Mark Yuly
#
# based on:
# energy_ex.py
# (c) 2016 SkuTek Instrumentation
# Author: D. Hunter
#
# versions:
#   0.1 09/22/16    - initial version based on histogram_ex.py
#   1.0 10/11/16  DH    - corrected usage because ARMED is not active high
#   1.1 10/25/16  DH    - updated logic for status read
#
# Capture energy data from the FemtoDAQ on inputs 0 and 1
# Create a CSV compatible text file with the data
#
# based on:
# decay_exp.py
# (c) 2016 Mark Yuly


import sys,time, datetime
from timeit import default_timer as timer
from FemtoLib import *          # import the Digitizer class
import Adafruit_BBIO.GPIO as GPIO

# from DAQfile import DataFile      # import the DataFile class

### GPIO parameters
GPIO_A = "GPIO0_22"  # input channel A
GPIO_B = "GPIO1_29"  # input channel B

### parameters for data capture
OFFSET0 = -12   #offset %
OFFSET1 = -20   #offest %

SIG_POL0 = INVERT   # ADC polarity
SIG_POL1 = INVERT   # ADC polarity
TRIG_POL = RISING   # Trigger polarity

BLR0 = ENABLE       # baseline restore
BLN_BLOCK0 = 100    # [samples] baseline blocking period
BLR1 = ENABLE       # baseline restore
BLN_BLOCK1 = 100    # [samples] baseline blocking period

PULSE_WIN = 100         # [samples] pulse height window
SIG_AVG0 = 4        # [samples] signal averaging time (QDC length)
```

```
SIG_AVG1 = 4        # [samples] signal averaging time (QDC length)
PT_DELAY = 100      # [samples] post trigger delay


# main routine
if __name__ == '__main__':
    if len(sys.argv) < 4:   # need run number and timeout parameter
        print 'Usage: decay_exp.py run_num t repeats'
        print ' run_num = starting run number'
        print ' t = time out value (milliseconds) [1-65535]'
        print ' repeats = number of times to repeat time out value for a given run \n'
        print 'Digital I/O:'
        print '  0 = (IN)  External Trigger'
        print '  1 = (IN)  Veto'
        print '  2 = (OUT) Armed'
        print '  3 = (OUT) Logging Busy'
        sys.exit()


    # convert run number and catch any errors
    try:
        run  = int(sys.argv[1])
    except:
        print 'Invalid starting run number'
        sys.exit()

    if (run < 0):
        print 'Invalid starting run number (must be >= 0)'
        sys.exit()


    # convert timeout and catch any errors
    try:
        TimeOut  = int(sys.argv[2])
    except:
        print 'Invalid timeout value (must be 1-65535)'
        sys.exit()

    if (TimeOut <= 0):
        print 'Invalid timeout value (must be 1-65535)'
        sys.exit()

    try:
        repeats  = int(sys.argv[3])
    except:
        print 'Invalid run number'
        sys.exit()

    if (repeats < 1):
        print 'Invalid run number (must be at least 1)'
        sys.exit()

    ##########################
    #  SET UP THE FEMTODAQ
    ##########################

    digi = Digitizer()  # create a digitizer object
    digi.WaitForReady() # wait for it to be ready
```

```
# read the firmware
fwStr = digi.GetFirmwareString()

# read the ADCtype from the digitizer
ADCtype = digi.IdentifyADC()
digi.InitADC()      # normal mode

# turn off data and pulse test mode in case they were on before
digi.DisableDataTest()
digi.DisableInternalPulseGenerator()

digi.SetChannelSignalPolarity(0,SIG_POL0)
digi.SetChannelSignalPolarity(1,SIG_POL1)

digi.SetChannelOffsetVoltage(0,OFFSET0)
digi.SetChannelOffsetVoltage(1,OFFSET1)

if BLR0:
    digi.EnableChannelBaselineRestore(0)
else:
    digi.DisableChannelBaselineRestore(0)

if BLR1:
    digi.EnableChannelBaselineRestore(1)
else:
    digi.DisableChannelBaselineRestore(1)

digi.SetChannelBaselineBlocking(0,BLN_BLOCK0)
digi.SetChannelBaselineBlocking(1,BLN_BLOCK1)

# set the signal averaging time for each channel
digi.SetChannelSignalAveragingTime(0,SIG_AVG0)
digi.SetChannelSignalAveragingTime(1,SIG_AVG1)

# set the post trigger delay
digi.SetPostTriggerDelay(PT_DELAY)

# set the pulse energy window
digi.SetPulseEnergyWindow(PULSE_WIN)

digi.EnableExternalTrigger()

digi.SetEnergyLogTimeout(TimeOut)

digi.EnableEnergyLogging()

digi.Initialize(False)  # Initialize w/o ADC init



print  'Short lived isotope-counting system acquisition'
print  'Digitizer firmware revision:', fwStr
print  'Initializing ADC',ADCtype


# open output file first time
outputfilename =  'run_'+str(run).rjust(4,'0')+'.dat'
```

```
        f = open(outputfilename, 'w')
        print  'Run '+str(run)+' started at: '+
datetime.datetime.now().strftime("%I:%M:%S%p on %B %d, %Y")
        print>>f,   'Run '+str(run)+' started at: '+
datetime.datetime.now().strftime("%I:%M:%S%p on %B %d, %Y")
        print 'okay ready'

        ###################################
        # Start the FPGA running when GPIO A
        # is triggered on the shot pulse from the
        # control room.  Record the start time.
        ###################################

        #GPIO.setup(GPIO_B,GPIO.IN)  #set GPIO A to be an input

        #GPIO.wait_for_edge(GPIO_B, GPIO.RISING)  # exits when it goes high, timeout in 1
minute

        start = time.time()             # start time (sec) laser shot
        events = 0



        for x in range(0, repeats):

            loop_start = time.time()    # iteration start (sec)

            # start a new capture
            digi.StartCapture()

            # poll until timeout or data ready
            bailOut = 656   # exit if > 65535 milliseconds

            i = 0
            while (i < bailOut):
                status = digi.GetEnergyLogStatus()

                # if data ready or timeout and no data
                if ((status & 0x0100) == 0x0100) or ((status & 0x00A0) == 0x00A0):
                    break
                time.sleep(0.1)
                sys.stdout.write('.')
                sys.stdout.flush()
                i = i + 1

            loop_stop = time.time() # iteration start (sec)

            ts = digi.GetEnergyLogTimeStamp()
            dt = digi.GetEnergyLogDeadTime()
            ec = digi.GetEnergyLogCount()
            events = events + ec

            # collect all of the values
            data_temp = digi.GetEnergyLog()
            for index,item in enumerate(data_temp):
                (tt,aa1,aa2)=item
                ts = tt   # get correct time stamp for last entry, GetEnergyLogTimeStamp
does not work?
```

```
            tt = tt+(loop_start-start)*100000000
            data_temp[index]=(tt,aa1,aa2)

        if (x==0):
            data = []
            data.extend(data_temp)
        else:
            data.extend(data_temp)

        print '\n\nClock Data Collection time = %10.6f seconds\n' % (loop_stop-start)
        print 'Status      : 0x%04X' % (status)
        print 'Time Stamp  : %d' % (ts)
        print 'Dead Time   : %d' % (dt)
        try:
            print '            : %.2f%%' % (100*(float(dt)/float(ts)))
        except:
            print '            : NaN'

        print 'Event Count : %d \n' % (ec)
        print 'Total Events : %d \n' % (events)

    stop = time.time()


    # write useful info to terminal
    print "\n\n++++++++++++++++++++++++++++++++"
    print  'Run ended at: ' + datetime.datetime.now().strftime("%I:%M:%S%p on %B %d,
%Y")
    print  'Clock Data Collection time = %10.6f seconds\n' % (stop-start)
    print 'Total Events : %d \n' % (events)


    # write out the data to a file
    print>>f, "\n\n++++++++++++++++++++++++++++++++"
    print>>f,  'Run ended at: ' + datetime.datetime.now().strftime("%I:%M:%S%p on %B
%d, %Y")
    print>>f,  'Clock Data Collection time = %10.6f seconds\n' % (stop-start)
    print>>f, 'Total Events : %d \n' % (events)


    # write to output file
    for s,a,b in data:
        #(s,a,b) = d
        print>>f, '%d   %d   %d' % (s,a,b)

    print >>f, 'Short lived isotope-counting system acquisition'
    f.close()

    status = digi.GetEnergyLogStatus()
    print 'Final Status: 0x%04X' % (status)

    # turn off pulse energy logging
    digi.DisableEnergyLogging()

    digi.close()        # release the SPI lines
    print 'Done'
```

Appendix C

CODE USED TO CONTROL THE PNEUMATIC VALVES

```
/*
  Web Server Demo
  thrown together by Randy Sarafan

 A simple web server that changes the page that is served, triggered by a
button press.

 Circuit:
 * Ethernet shield attached to pins 10, 11, 12, 13
 * Connect a button between Pin D2 and 5V
 * Connect a 10K resistor between Pin D2 and ground

 Based almost entirely upon Web Server by Tom Igoe and David Mellis

 Edit history:
 created 18 Dec 2009
 by David A. Mellis
 modified 4 Sep 2010
 by Tom Igoe

 */

#include <SPI.h>
#include <Ethernet.h>

String quote = String('"');
bool valveState[] = {false,false,false,false};
int valvePins[] = {4,5,6,7};
int incoming =0;
String msg ="";
// Enter a MAC address and IP address for your controller below.
// The IP address will be dependent on your local network:
byte mac[] = { 0x00, 0xAA, 0xBB, 0xCC, 0xDA, 0x02 };
IPAddress ip(192,168,1,3); //<<< ENTER YOUR IP ADDRESS HERE!!!

// Initialize the Ethernet server library
// with the IP address and port you want to use
// (port 80 is default for HTTP):
EthernetServer server(80);

void setup()
{
  Serial.begin(9600);
  // start the Ethernet connection and the server:
  Ethernet.begin(mac, ip);
  server.begin();

  for(int i=0;i<4;i++){
    pinMode(valvePins[i], OUTPUT);
  }
}
```

```
   void loop()
   {
     // listen for incoming clients
     EthernetClient client = server.available();
     if (client) {

       // an http request ends with a blank line
       boolean currentLineIsBlank = true;
       while (client.connected()) {
         if (client.available()) {
           char c = client.read();

           if(c == '$'){
             incoming = 3;
           }

           if(incoming > 0){
             msg+=c;
             incoming-=1;
           }

           if (c == '\n' && currentLineIsBlank) {
             updateValves(msg);
             msg="";
             // send a standard http response header
             client.println("HTTP/1.1 200 OK");
             client.println("Content-Type: text/html");
             client.println();

             client.println("<HTML>");
             client.println("<HEAD>");
             client.println("<TITLE>Valve Control</TITLE>");
             client.println("</HEAD>");
             client.println("<style>");
             client.println(".btn{width: 20%; height: 20%;font-
size:2.2vw;position:absolute;border:none;font-family:sans-serif;}");
             client.println(".btn:hover{box-shadow: 12px 16px 0 rgba(0,0,0,0.24),
0 17px 50px 0 rgba(0,0,0,0.19);cursor: pointer;}");
             client.println(".btn1{left:10%; top:10%}");
             client.println(".btn2{left:40%; top:10%}");
             client.println(".btn3{left:70%; top:10%}");
             client.println(".btn4{left:50%; top:38%; transform: translateX(-
50%); background-color:red;border-radius:50%; width: 30vw; height:30vw}");

             client.println("</style>");
             client.println("<BODY>");


             //serves a different version of a website depending on whether or
not the button
             //connected to pin 2 is pressed.

             if(valveState[0]==true){
                 client.println("<button class='btn btn1'
onClick="+quote+"window.location.href='$10'"+quote+" style='background-
color:green;'>Detector/Foreline <br> Open</button>");
             }
             else if(valveState[0]==false){
```

```
                client.println("<button class='btn btn1'
onClick="+quote+"window.location.href='$11'"+quote+" style='background-
color:yellow;'>Detector/Foreline <br> closed</button>");
              }

              if(valveState[1]==true){
                  client.println("<button class='btn btn2'
onClick="+quote+"window.location.href='$20'"+quote+" style='background-
color:green;'>Foreline <br> Open</button>");
              }
              else if(valveState[1]==false){
                 client.println("<button class='btn btn2'
onClick="+quote+"window.location.href='$21'"+quote+" style='background-
color:yellow;'>Foreline <br> Closed</button>");
              }

              if(valveState[2]==true){
                  client.println("<button class='btn btn3'
onClick="+quote+"window.location.href='$30'"+quote+" style='background-
color:green;'>Accelerator <br> Open</button>");
              }
              else if(valveState[2]==false){
                 client.println("<button class='btn btn3'
onClick="+quote+"window.location.href='$31'"+quote+" style='background-
color:yellow;'>Accelerator <br> Closed</button>");
              }

              if(valveState[3]==true){
                  client.println("<button class='btn btn4'
onClick="+quote+"window.location.href='$40'"+quote+">UNDETONATE</button>");
              }
              else if(valveState[3]==false){
                 client.println("<button class='btn btn4'
onClick="+quote+"window.location.href='$41'"+quote+"><b>DETONATE</b></button>rando
m characters can go here");
              }

              client.println("</BODY>");
              client.println("</HTML>");


              break;
            }
            if (c == '\n') {
              // you're starting a new line
              currentLineIsBlank = true;
            }
            else if (c != '\r') {
              // you've gotten a character on the current line
              currentLineIsBlank = false;
            }

          }
        }
        // give the web browser time to receive the data
        delay(1);
        // close the connection:
        client.stop();
      }
```

```
}

void updateValves(String message){
  //Serial.println(valveState[0]);
  int valve = int(message[1])-48;
  int stateNum = int(message[2]-48);
  bool state;
  if (stateNum ==1){
    state = true;
  }
  else state = false;
  Serial.print(message);
 // Serial.println(valvePins[valve-1]);
  //Serial.println(state);
  digitalWrite(valvePins[valve-1], state);
  valveState[valve-1]=state;

}
```

R e f e r e n c e s

[1] I. Thompson, F. Nunes, *Nuclear Reactions in Astrophysics* (Cambridge University Press, Cambridge, 2009) p. 4-9.

[2] National Nuclear Data Center, information extracted from the Chart of Nuclides database, http://www.nndc.bnl.gov/chart/.

[3] M. Asplund et al., Astrophys. J. **644**, 229 (2006).

[4] C. Grupen, *Big Bang Nucleosynthesis* (Springer Nature Switzerland AG, 2020) p. 223.

[5] R. Nakamura, M. Hashimoto, R. Ichimasa, K. Arai, International Journal of Modern Physics E **26**, 1 (2017).

[6] K. Cook, B.S. thesis, Houghton College, 2019.

[7] E. Moses, Multi-megajoule NIF: Ushering in a New Era in High Energy Density Science, (Lawrence Livermore National Laboratory, 2008).

[8] Laboratory for Laser Energetics Report, DOE/NA/28302-992, 2011.

[9] L. Gresh, *Inertial Confinement Fusion: An Introduction* (University of Rochester, Laboratory for Laser Energetics, 2008), p. 21-31.

[10] L. J. Waxer, et al., Optics and Photonics News **16**, 30 (2005).

[11] M. Yuly, S. Padalino, E. Bruce, K. Cook, and S. Hull, "Measuring Low Energy Nuclear Cross Sections using ICF" in Nuclear and Plasma Diagnostics for the EP-OMEGA and MTW Laser Systems, LLE Proposal, 2018 (unpublished).

[12] A.J. Koning, S. Hilaire and M.C. Duijvestijn, "TALYS-1.0", Proceedings of the International Conference on Nuclear Data for Science and Technology, April 22-27, 2007, Nice, France, editors. O.Bersillon, F.Gunsing, E.Bauge, R.Jacqmin, and S.Leray, EDP Sciences, 211 (2008).

[13] S.N. Abramovich, B.Y. Guzhovskij, V.A. Zherebtsov, and A.G. Zvenigorodskij, International Nuclear Data Committee Report INDC(CCP)-326/L+F, 1991.

[14] M. Yuly, S. Padalino, T. Kowalewski, S. Ferri, and S. Raymond, "Inertial Confinement Fusion as a Tool to Study Fundamental Nuclear Science, the rapid isotope-counting system (RICS) using a hollow box phoswich detector" in Nuclear and Plasma Diagnostics for the EP-OMEGA and MTW Laser Systems, LLE Proposal, 2019 (unpublished).

[15] M. Yuly, S. Padalino, M. Coats, and K. Cook, "Progress toward using ICF to measure light-ion nuclear cross sections" in Nuclear and Plasma Diagnostics for the EP-OMEGA and MTW Laser Systems, LLE Proposal, 2017 (unpublished).

[16] M. Yuly, S. Padalino, M. Christensen, and J. Bowman, "Progress toward using ICF to measure light-ion nuclear cross sections" in Nuclear and Plasma Diagnostics for the EP-OMEGA and MTW Laser Systems, LLE Proposal, 2020 (unpublished).

[17] T. Kowalewski, B.S. thesis, Houghton College, 2021.

[18] M. Yuly, S. Padalino, A. Brown, M. Christensen, and M. Condie, "Trapping and detecting trace radioactive isotopes produced in ICF implosions" in Nuclear and Plasma Diagnostics for the EP-OMEGA and MTW Laser Systems, LLE Proposal, 2021 (unpublished).

[19] Eljen Technology. Products: Plastic Scintillators [Online]. 2021. http://eljentechnology.com/products/plastic-scintillators [Jan. 2022].

[20] N. Gindling, K. Andersen, E. Parker, and S. Padalino, "Using a ^{64}Cu source to test SLICS" in Nuclear and Plasma Diagnostics for the EP-OMEGA and MTW Laser Systems, LLE Proposal, 2021 (unpublished).

[21] F. James, CERN Report No. CERN-D-506, 1994 (unpublished).

[22] Rene Brun and Fons Rademakers, Nucl. Inst. & Meth. In Phys. Res. A **389**, 81-86 (1997)